MitoEAGLE preprint 2017-10-20(11)

The protonmotive force and respiratory control:

Building blocks of mitochondrial physiology

Part 1.

http://www.mitoeagle.org/index.php/MitoEAGLE_preprint_2017-09-21

Preprint version 10 (2017-10-15)

MitoEAGLE Network

Corresponding author: Gnaiger E

Contributing co-authors

Ahn B, Alves MG, Amati F, Åsander Frostner E, Bailey DM, Battino M, Beard DA, Ben-Shachar D, Bishop D, Breton S, Brown GC, Brown RA, Buettner GR, Carvalho E, Cervinkova Z, Chicco AJ, Coen PM, Collins JL, Crisóstomo L, Davis MS, Dias T, Distefano G, Doerrier C, Ehinger J, Elmer E, Fell DA, Ferko M, Ferreira JCB, Filipovska A, Fisher J, Garcia-Roves PM, Garcia-Souza LF, Genova ML, Gonzalo H, Goodpaster BH, Gorr TA, Han J, Harrison DK, Hellgren KT, Hernansanz P, Holland O, Hoppel CL, Iglesias-Gonzalez J, Irving BA, Iyer S, Jackson CB, Jansen-Dürr P, Jespersen NR, Jha RK, Kaambre T, Kane DA, Kappler L, Keijer J, Komlodi T, Kopitar-Jerala N, Krako Jakovljevic N, Kuang J, Labieniec-Watala M, Lai N, Laner V, Lee HK, Lemieux H, Lerfall J, Lucchinetti E, MacMillan-Crow LA, Makrecka-Kuka M, Meszaros AT, Moisoi N, Molina AJA, Montaigne D, Moore AL, Murray AJ, Newsom S, Nozickova K, O'Gorman D, Oliveira PF, Oliveira PJ, Orynbayeva Z, Pak YK, Palmeira CM, Patel HH, Pesta D, Petit PX, Pichaud N, Pirkmajer S, Porter RK, Pranger F, Prochownik EV, Radenkovic F, Reboredo P, Renner-Sattler K, Robinson MM, Rohlena J, Røsland GV, Rossiter HB, Salvadego D, Scatena R, Schartner M, Scheibye-Knudsen M, Schilling JM, Schlattner U, Schoenfeld P, Scott GR, Singer D, Sobotka O, Spinazzi M, Stier A, Stocker R, Sumbalova Z, Suravajhala P, Tanaka M, Tandler B, Tepp K,

Tomar D, Towheed A, Trivigno C, Tronstad KJ, Trougakos IP, Tyrrell DJ, Velika B, Vendelin M, Vercesi AE, Victor VM, Ward ML, Watala C, Wei YH, Wieckowski MR, Wohlwend M, Wolff J, Wuest RCI, Zaugg K, Zaugg M, Zorzano A

Supporting co-authors:

Arandarčikaitė O, Bakker BM, Bernardi P, Boetker HE, Borsheim E, Borutaitė V, Bouitbir J, Calabria E, Calbet JA, Chaurasia B, Clementi E, Coker RH, Collin A, Das AM, De Palma C, Dubouchaud H, Duchen MR, Durham WJ, Dyrstad SE, Engin AB, Fornaro M, Gan Z, Garlid KD, Garten A, Gourlay CW, Granata C, Haas CB, Haavik J, Haendeler J, Hand SC, Hepple RT, Hickey AJ, Hoel F, Kainulainen H, Keppner G, Khamoui AV, Klingenspor M, Koopman WJH, Kowaltowski AJ, Krajcova A, Lenaz G, Malik A, Markova M, Mazat JP, Menze MA, Methner A, Muntané J, Muntean DM, Neuzil J, Oliveira MT, Pallotta ML, Parajuli N, Pettersen IKN, Pulinilkunnil T, Ropelle ER, Salin K, Sandi C, Sazanov LA, Siewiera K, Silber AM, Skolik R, Smenes BT, Soares FAA, Sokolova I, Sonkar VK, Stankova P, Swerdlow RH, Szabo I, Trifunovic A, Thyfault JP, Tretter L, Vieyra A, Votion DM, Williams C

Updates:

http://www.mitoeagle.org/index.php/MitoEAGLE_preprint_2017-09-21

Correspondence: Gnaiger E
Department of Visceral, Transplant and Thoracic Surgery, D. Swarovski Research Laboratory, Medical University of Innsbruck, Innrain 66/4, A-6020 Innsbruck, Austria
Email: erich.gnaiger@i-med.ac.at
Tel: +43 512 566796, Fax: +43 512 566796 20

This manuscript on 'The protonmotive force and respiratory control' is a position statement in the frame of COST Action CA15203 MitoEAGLE. The list of co-authors evolved from MitoEAGLE Working Group Meetings and a ***bottom-up*** *spirit of COST in phase 1: This is an open invitation to scientists and students to join as co-authors, to provide a balanced view on mitochondrial respiratory control, a fundamental introductory presentation of the concept of the protonmotive force, and a consensus statement on reporting data of mitochondrial respiration in terms of metabolic flows and fluxes. We plan a series of follow-up reports by the expanding MitoEAGLE Network, to increase the scope of recommendations on harmonization and facilitate global communication and collaboration.*

*Phase 2****:*** *MitoEAGLE preprint (Versions 01 – 10): We continue to invite comments and suggestions on the, particularly if you are an* ***early career investigator adding an open future-oriented perspective****, or an* ***established scientist providing a balanced historical basis****. Your critical input into the quality of the manuscript will be most welcome, improving our aims to be educational, general, consensus-oriented, and practically helpful for students working in mitochondrial respiratory physiology.*

Phase 3 (2017-11-11): Manuscript submission to a preprint server, such as BioRxiv. We want to invite further opinion leaders: *To join as a co-author, please feel free to focus on a particular section in terms of direct input and references, contributing to the scope of the manuscript from the perspective of your expertise. Your comments will be largely posted on the discussion page of the MitoEAGLE preprint website.*

If you prefer to submit comments in the format of a referee's evaluation rather than a contribution as a co-author, I will be glad to distribute your views to the updated list of co-authors for a balanced response. We would ask for your consent on this open bottom-up policy.

*Phase 4: We organize a MitoEAGLE session linked to our series of reports at the MiP*conference *Nov 2017 in Hradec Kralove in close association with the MiPsociety (where you hopefully will attend) and at EBEC 2018 in Budapest.*

» http://www.mitoeagle.org/index.php/MiP2017_Hradec_Kralove_CZ

I thank you in advance for your feedback.
With best wishes,

Erich Gnaiger
Chair Mitochondrial Physiology Society - http://www.mitophysiology.org
Chair COST Action MitoEAGLE - http://www.mitoeagle.org
Medical University of Innsbruck, Austria

Contents

Abstract

Clarity of concept and consistency of nomenclature are key trademarks of a research field. These trademarks facilitate effective transdisciplinary communication, education, and ultimately further discovery. As the knowledge base and importance of mitochondrial physiology to human health expand, the necessity for harmonizing nomenclature concerning mitochondrial respiratory states and rates has become increasingly apparent. Peter Mitchell's concept of the protonmotive force establishes the links between electrical and chemical components of energy transformation and coupling in oxidative phosphorylation. This unifying concept provides the framework for developing a consistent nomenclature for mitochondrial physiology and bioenergetics. Herein, we follow IUPAC guidelines on general terms of physical chemistry, extended by the concepts of open systems and irreversible thermodynamics. We align the nomenclature of classical bioenergetics on respiratory states with a concept-driven constructive terminology to address the meaning of each respiratory state. Furthermore, we suggest uniform standards for the evaluation of respiratory states that will ultimately support the development of databases of mitochondrial respiratory function in species, tissues and cells studied under diverse physiological and experimental conditions. In this position statement, in the frame of COST Action CA15203 MitoEAGLE, we endeavour to provide a balanced view on mitochondrial respiratory control, a fundamental introductory presentation of the concept of the protonmotive force, and a critical discussion on reporting data of mitochondrial respiration in terms of metabolic flows and fluxes.

Keywords: Mitochondrial respiratory control, coupling control, mitochondrial preparations, protonmotive force, chemiosmotic theory, oxidative phosphorylation, OXPHOS, efficiency, electron transfer, ET; proton leak, LEAK, residual oxygen consumption, ROX, State 2, State 3, State 4, normalization, flow, flux

Box 1:

In brief: mitochondria and Bioblasts

* Does the public expect biologists to understand Darwin's theory of evolution?
* Do students expect that researchers of bioenergetics can explain Mitchell's theory of chemiosmotic energy transformation?

Mitochondria were described for the first time in 1857 by Rudolph Albert Kölliker as granular structures or 'sarkosomes' *(a reference is needed)*. In 1886 *(a reference is needed)* Richard Altmann called them 'bioblasts' (published 1894). The word 'mitochondrium' (Greek mitos: thread; chondros: granule) was introduced by Carl Benda (1898). Mitochondria are the oxygen consuming electrochemical generators which evolved from endosymbiotic bacteria (Margulis 1970; Lane 2005). The bioblasts of Richard Altmann (1894) included not only the mitochondria as presently defined, but also symbiotic and free-living bacteria.

We now recognize mitochondria as dynamic organelles with a double membrane that are contained within eukaryotic cells. The mitochondrial inner membrane (mtIM) shows dynamic tubular to disk-shaped cristae that separate the mitochondrial matrix, *i.e.* the internal mitochondrial compartment, and the intermembrane space; the latter being enclosed by the mitochondrial outer membrane (mtOM). Mitochondria are the structural and functional elemental units of cell respiration. Cell respiration is the consumption of oxygen by electron transfer coupled to electrochemical proton translocation across the mtIM. In the process of oxidative phosphorylation (OXPHOS), the reduction of O_2 is electrochemically coupled to the transformation of energy in the form of adenosine triphosphate (ATP; Mitchell 2011). These powerhouses of the cell contain the machinery of the OXPHOS-pathway, including transmembrane respiratory complexes (*i.e.* proton pumps with FMN, Fe-S and cytochrome *b*, *c*, aa_3 redox systems); alternative dehydrogenases and oxidases; the coenzyme ubiquinone (Q); ATP synthase; the enzymes of the tricarboxylic acid cycle and the fatty acid oxidation enzymes; transporters of ions, metabolites and co-factors; and mitochondrial kinases related to energy transfer pathways. The mitochondrial proteome comprises over 1,200 proteins

198 (MITOCARTA), mostly encoded by nuclear DNA (nDNA), with a variety of functions, many
199 of which are relatively well known (*e.g.* apoptosis-regulating proteins), while others are still
200 under investigation, or need to be identified (*e.g.* alanine transporter).

201 Mitochondria typically maintain several copies of their own genome (hundred to
202 thousands per cell; Cummins 1998), which is almost exclusively maternally inherited (White *et*
203 *al.* 2008) and known as mitochondrial DNA (mtDNA). One exception to strictly maternal
204 inheritance in animals is found in bivalves (Breton *et al.* 2007). mtDNA is 16.5 Kb in length,
205 contains 13 protein-coding genes for subunits of the transmembrane respiratory Complexes CI,
206 CIII, CIV and ATP synthase, and also encodes 22 tRNAs and the mitochondrial 16S and 12S
207 rRNA. The mitochondrial genome is both regulated and supplemented by nuclear-encoded
208 mitochondrial targeted proteins. Evidence has accumulated that additional gene content is
209 encoded in the mitochondrial genome, *e.g.* microRNAs, piRNA, smithRNAs, repeat associated
210 RNA, and even additional proteins (Duarte *et al.* 2014; Lee *et al.* 2015; Cobb *et al.* 2016).

211 The mtIM contains the non-bilayer phospholipid cardiolipin, which is not present in any
212 other eukaryotic cellular membrane. Cardiolipin promotes the formation of respiratory
213 supercomplexes, which are supramolecular assemblies based upon specific, though dynamic,
214 interactions between individual respiratory complexes (Greggio *et al.* 2017; Lenaz *et al.* 2017).
215 Membrane fluidity is an important parameter influencing functional properties of proteins
216 incorporated in the membranes (Waczulikova *et al.* 2007). There is a constant crosstalk between
217 mitochondria and the other cellular components, maintaining cellular mitostasis through
218 regulation at both the transcriptional and post-translational level, and through cell signalling
219 including proteostatic (e.g. the ubiquitin-proteasome and autophagy-lysosome pathways) and
220 genome stability modules thoughout the cell cycle or even cell death, contributing to
221 homeostatic regulation in response to varying energy demands and stress (Quiros *et al.* 2016).
222 In addition to mitochondrial movement along the microtubules, mitochondrial morphology can
223 change in response to the energy requirements of the cell via processes known as fusion and

fission, through which mitochondria can communicate within a network, and in response to intracellular stress factors causing swelling and ultimately permeability transition.

Mitochondrial dysfunction is associated with a wide variety of genetic and degenerative diseases. Robust mitochondrial function is supported by physical exercise and caloric balance, and is central for sustained metabolic health throughout life. Therefore, a better understanding of mitochondrial physiology will improve our understanding of the etiology of disease, the diagnostic repertoire of mitochondrial medicine, with a focus on protective medicine, lifestyle and healthy aging.

Abbreviation: mt, as generally used in mtDNA. Mitochondrion is singular and mitochondria is plural.

'*For the physiologist, mitochondria afforded the first opportunity for an experimental approach to structure-function relationships, in particular those involved in active transport, vectorial metabolism, and metabolic control mechanisms on a subcellular level*' (Ernster and Schatz 1981).

---

1. Introduction

Mitochondria are the powerhouses of the cell with numerous physiological, molecular, and genetic functions (**Box 1**). Every study of mitochondrial function and disease is faced with **E**volution, **A**ge, **G**ender and sex, **L**ifestyle, and **E**nvironment (EAGLE) as essential background conditions intrinsic to the individual patient or subject, cohort, species, tissue and to some extent even cell line. As a large and highly coordinated group of laboratories and researchers, the mission of the global MitoEAGLE Network is to generate the necessary scale, type, and quality of consistent data sets and conditions to address this intrinsic complexity. Harmonization of experimental protocols and implementation of a quality control and data management system is required to interrelate results gathered across a spectrum of studies and to generate a rigorously monitored database focused on mitochondrial respiratory function. In this way,

researchers within the same and across different disciplines will be positioned to compare their findings to an agreed upon set of clearly defined and accepted international standards.

Reliability and comparability of quantitative results depend on the accuracy of measurements under strictly-defined conditions. A conceptually defined framework is also required to warrant meaningful interpretation and comparability of experimental outcomes carried out by research groups at different institutes. With an emphasis on quality of research, collected data can be useful far beyond the specific question of a particular experiment. Enabling meta-analytic studies is the most economic way of providing robust answers to biological questions (Cooper *et al.* 2009). Vague or ambiguous jargon can lead to confusion and may relegate valuable signals to wasteful noise. For this reason, measured values must be expressed in standardized units for each parameter used to define mitochondrial respiratory function. Standardization of nomenclature and definition of technical terms is essential to improve the awareness of the intricate meaning of a divergent scientific vocabulary. The focus on the protonmotive force, coupling states, and fluxes through metabolic pathways of aerobic energy transformation in mitochondrial preparations is a first step in the attempt to generate a harmonized and conceptually-oriented nomenclature in bioenergetics and mitochondrial physiology. Coupling states of intact cells and respiratory control by fuel substrates and specific inhibitors of respiratory enzymes will be reviewed in subsequent communications.

2. Respiratory coupling states in mitochondrial preparations

> '*Every professional group develops its own technical jargon for talking about matters of critical concern ... People who know a word can share that idea with other members of their group, and a shared vocabulary is part of the glue that holds people together and allows them to create a shared culture*' (Miller 1991).

Mitochondrial preparations are defined as either isolated mitochondria, or tissue and cellular preparations in which the barrier function of the plasma membrane is disrupted. The plasma membrane separates the cytosol, nucleus, and organelles (the intracellular compartment) from the environment of the cell. The plasma membrane consists of a lipid bilayer, embedded proteins, and attached organic molecules that collectively control the selective permeability of ions, organic molecules, and particles across the cell boundary. The intact plasma membrane, therefore, prevents the passage of many water-soluble mitochondrial substrates, such as succinate or adenosine diphosphate (ADP), that are required for the analysis of respiratory capacity at kinetically-saturating concentrations, thus limiting the scope of investigations into mitochondrial respiratory function in intact cells. The cholesterol content of the plasma membrane is high compared to mitochondrial membranes. Therefore, mild detergents, such as digitonin and saponin, can be applied to selectively permeabilize the plasma membrane by interaction with cholesterol and allow free exchange of cytosolic components with ions and organic molecules of the immediate cell environment, while maintaining the integrity and localization of organelles, cytoskeleton, and the nucleus. Application of optimum concentrations of these mild detergents leads to the complete loss of cell viability, tested by nuclear staining, while mitochondrial function remains intact, as shown by an unaltered respiration rate of isolated mitochondria after the addition of such low concertations of digitonin and saponin. In addition to mechanical permeabilization during homogenization of fresh tissue, saponin may be applied to ensure permeabilization of all cells. Crude homogenate and cells permeabilized in the respiration chamber contain all components of the cell at highly diluted concentrations. All mitochondria are retained in chemically-permeabilized mitochondrial preparations and crude tissue homogenates. In the preparation of isolated mitochondria, the cells or tissues are homogenized, and the mitochondria are separated from other cell fractions and purified by differential centrifugation, entailing the loss of a significant fraction of

mitochondria. The term mitochondrial preparation does not include further fractionation of mitochondrial components, as well as submitochondrial particles.

2.1. Three coupling states of mitochondrial preparations and residual oxygen consumption

Respiratory capacities in coupling control states: To extend the classical nomenclature on mitochondrial coupling states (Section 2.4) by a concept-driven terminology that incorporates explicit information on the nature of the respiratory states, the terminology must be general and not restricted to any particular experimental protocol or mitochondrial preparation (Gnaiger 2009). We focus primarily on the conceptual 'why', along with clarification of the experimental 'how'. In the following section, the concept-driven terminology is explained and coupling states are defined. We define respiratory capacities, comparable to channel capacity in information theory (Schneider 2006), as the upper bound of the rate of respiration measured in defined coupling and electron transfer-pathway (ET-pathway) control states. To provide a diagnostic reference for respiratory capacities of core energy metabolism, the capacity of *oxidative phosphorylation*, OXPHOS, is measured at kinetically-saturating concentrations of ADP and inorganic phosphate, P_i. The *oxidative* ET-capacity reveals the limitation of OXPHOS-capacity mediated by the *phosphorylation*-pathway. The ET- and phosphorylation-pathways comprise coupled segments of the OXPHOS-pathway. ET-capacity is measured as noncoupled respiration by application of *external uncouplers*. The contribution of *intrinsically uncoupled* oxygen consumption is most easily studied in the absence of ADP, *i.e.* by not stimulating phosphorylation, or by inhibition of the phosphorylation-pathway. The corresponding states are collectively classified as LEAK-states, when oxygen consumption compensates mainly for the proton leak (**Table 1**). Different coupling states are induced by (*1*) adding ADP or P_i, (*2*) inhibiting the phosphorylation-pathway, and (*3*) performing uncoupler titrations, while maintaining a defined ET-pathway state with constant fuel substrates and ET inhibitors (**Fig. 1**).

Kinetic control: Coupling control states are established in the study of mitochondrial preparations to obtain reference values for various output variables. Physiological conditions *in vivo* may deviate substantially from these experimentally obtained states. Since kinetically-saturating concentrations, *e.g.* of ADP or oxygen, may not apply to physiological intracellular conditions, relevant information is obtained in studies of kinetic responses to conditions intermediate between the LEAK state at zero [ADP] and the OXPHOS-state at saturating [ADP], or of respiratory capacities in the range between kinetically-saturating [O_2] and anoxia (Gnaiger 2001).

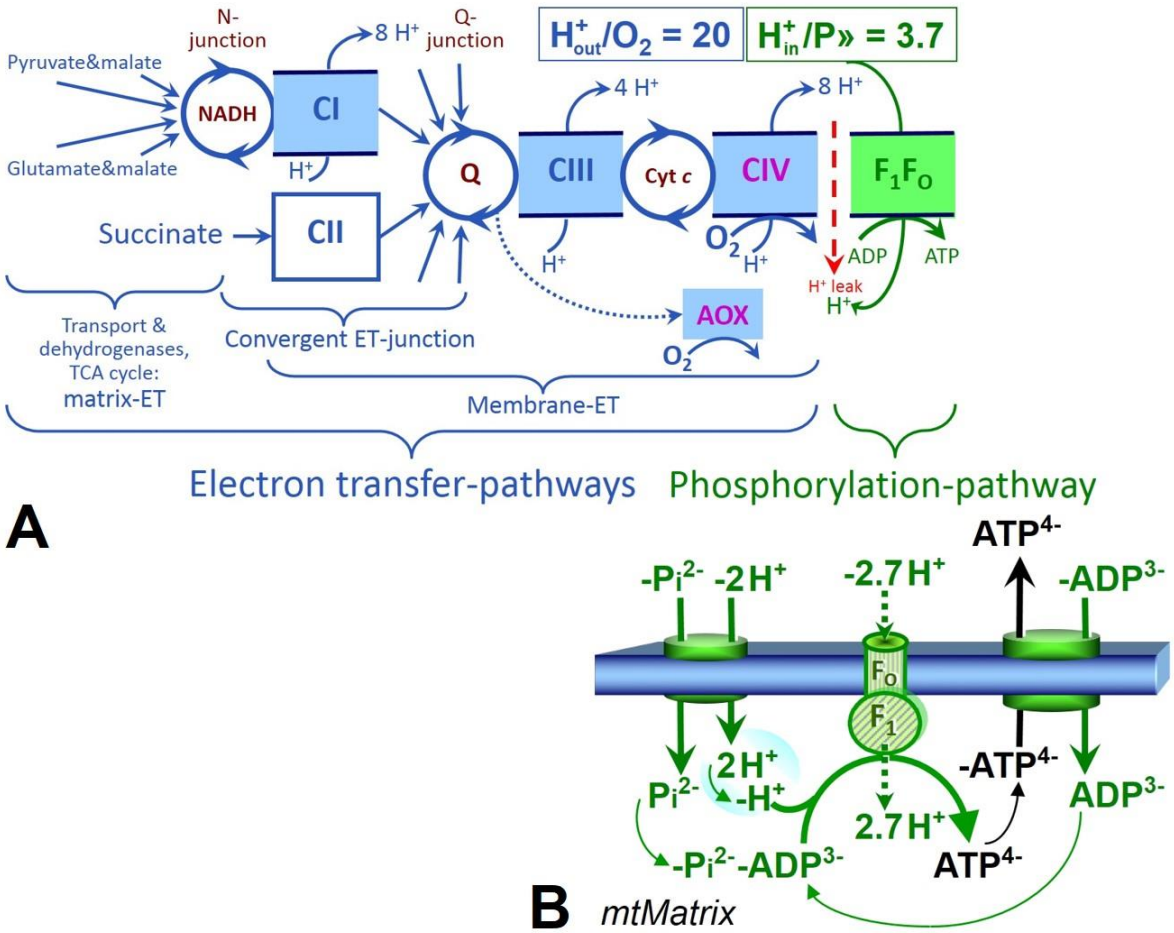

Fig. 1. The oxidative phosphorylation-pathway, OXPHOS-pathway. (A) Electron transfer, ET, coupled to phosphorylation. Multiple convergent ET-pathways are shown from NADH and succinate; additional arrows indicate electron entry through electron transferring flavoprotein, glycerophosphate dehydrogenase, dihydro-orotate dehydrogenase, choline dehydrogenase, and sulfide-ubiquinone oxidoreductase. The branched pathway of oxygen consumption by alternative quinol oxidase (AOX) is

indicated by the dotted arrow. The H^+_{out}/O_2 ratio is the outward proton flux from the matrix space divided by catabolic O_2 flux in the NADH-pathway. The $H^+_{in}/P»$ ratio is the inward proton flux from the inter-membrane space divided by the flux of phosphorylation of ADP to ATP. Due to proton leak and slip these are not fixed stoichiometries. (**B**) Phosphorylation-pathway catalyzed by the F_1F_O ATP synthase, adenine nucleotide translocase, and inorganic phosphate transporter. The $H^+_{in}/P»$ stoichiometry is the sum of the coupling stoichiometry in the ATP synthase reaction (-2.7 H^+ from the intermembrane space, 2.7 H^+ to the matrix) and the proton balance in the translocation of ADP^{2-}, ATP^{3-} and P_i^{2-}. See Eqs. 3 and 4 for further explanation. Modified from (A) Lemieux *et al*. (2017) and (B) Gnaiger (2014).

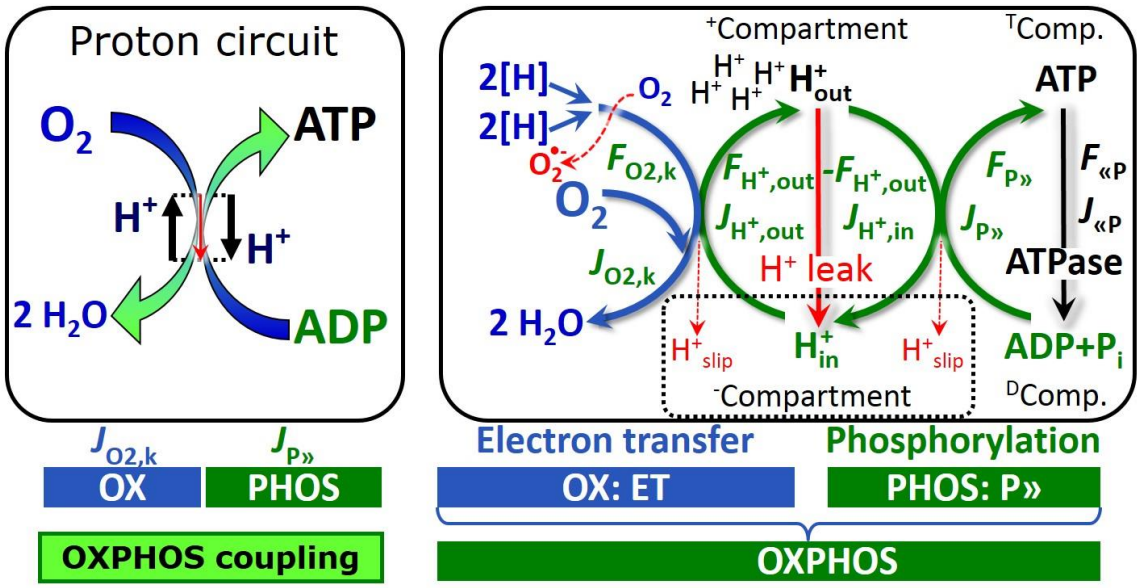

Fig. 2. The proton circuit and coupling in oxidative phosphorylation (OXPHOS). Oxygen flux, $J_{O2,k}$, through the catabolic electron transfer-pathway k is coupled to flux through the phosphorylation-pathway of ADP to ATP, $J_{P»}$, by the proton pumps of the ET-pathway, pushing the outward proton flux, $J_{H+,out}$, and generating the output protonmotive force, $F_{H+,out}$. ATP synthase is coupled to inward proton flux, $J_{H+,in}$, to phosphorylate ADP+P_i to ATP, driven by the input protonmotive force, $F_{H+,in} = -F_{H+,out}$. 2[H] indicates the reduced hydrogen equivalents of fuel substrates that provide the chemical input force, $F_{O2,k}$ [kJ/mol O_2], of the catabolic reaction k with oxygen (Gibbs energy of reaction per mole O_2 consumed in reaction k), typically in the range of -460 to -480 kJ/mol. The output force is given by the phosphorylation potential difference (ADP phosphorylated to ATP), $F_{P»}$, which varies *in vivo* ranging from about 48 to 62 kJ/mol under physiological conditions (Gnaiger 1993a). Fluxes, J_B, and forces, F_B, are expressed in either chemical units, [mol·s^{-1}·m^{-3}] and [J·mol^{-1}] respectively, or electrical units, [C·s^{-1}·m^{-3}] and [J·C^{-1}]

361 respectively, per volume, V [m^3], of the system. The system defined by the boundaries shown as a full
362 black line is not a black box, but is analysed as a compartmental system. The negative compartment
363 ($^-$Compartment, enclosed by the dotted line) is the matrix space, separated from the positive
364 compartment ($^+$Compartment) by the mtIM. ADP+P_i and ATP are the substrate- and product-
365 compartments (scalar ADP and ATP compartments, ^{D}Comp. and ^{T}Comp.), respectively. Chemical
366 potentials of all substrates and products involved in the scalar reactions are measured in the
367 $^+$Compartment for calculation of the scalar forces $F_{O2,k}$ and $F_{P»} = -F_{«P}$ (**Box 2**). Modified from Gnaiger
368 (2014).
369
370 **Phosphorylation, P»:** *Phosphorylation* in the context of OXPHOS is defined as
371 phosphorylation of ADP to ATP. On the other hand, the term phosphorylation is used generally
372 in many different contexts, *e.g.* protein phosphorylation. This justifies consideration of a
373 symbol more discriminating and specific than P as used in the P/O ratio (phosphate to atomic
374 oxygen ratio; O = 0.5 O_2), where P indicates phosphorylation of ADP to ATP or GDP to GTP.
375 We propose the symbol P» for the endergonic direction of phosphorylation ADP→ATP, and
376 likewise the symbol «P for the corresponding exergonic hydrolysis ATP→ADP (**Fig. 2; Box**
377 **3**). ATP synthase is the proton pump of the phosphorylation-pathway (**Fig. 1B**). P» may also
378 involve substrate-level phosphorylation as part of the tricarboxylic acid cycle (succinyl-CoA
379 ligase) and phosphorylation of ADP catalyzed by phosphoenolpyruvate carboxykinase,
380 adenylate kinase, creatine kinase, hexokinase and nucleoside diphosphate kinase (NDPK).
381 Kinase cycles are involved in intracellular energy transfer and signal transduction for regulation
382 of energy flux. In isolated mammalian mitochondria ATP production catalyzed by adenylate
383 kinase, 2ADP ↔ ATP + AMP, proceeds without fuel substrates in the presence of ADP
384 (Komlódi and Tretter 2017). $J_{P»}/J_{O2,k}$ (P»/O_2) is two times the 'P/O' ratio of classical
385 bioenergetics. The effective P»/O_2 ratio is diminished by: (*1*) the proton leak across the mtIM
386 from low pH in the $^+$Compartment to high pH in the $^-$Compartment; (*2*) cycling of other cations;

387 (*3*) proton slip in the proton pumps when a proton effectively is not pumped; and (*4*) electron
388 leak in the univalent reduction of oxygen (O_2; dioxygen) to superoxide anion radical ($O_2^{\bullet-}$).
389
390 **Table 1. Coupling states and residual oxygen consumption in mitochondrial**
391 **preparations in relation to respiration- and phosphorylation-rate, $J_{O2,k}$ and $J_{P»}$,**
392 **and protonmotive force, $F_{H+,out}$.** Coupling states are established at kinetically-
393 saturating concentrations of fuel substrates and O_2.

State	$J_{O2,k}$	$J_{P»}$	$F_{H+,out}$	Inducing factors	Limiting factors
LEAK	*L*; low proton leak-dependent respiration	0	max.	Proton leak, slip, and cation cycling	$J_{P»}$ = 0: (*1*) without ADP, L_N; (*2*) max. ATP/ADP ratio, L_T; or (*3*) inhibition of the phosphorylation-pathway, L_{Omy}
OXPHOS	*P*; high ADP-stimulated respiration	max.	high	Kinetically-saturating [ADP] and [P_i]	$J_{P»}$ by phosphorylation-pathway; or $J_{O2,k}$ by ET-capacity
ET	*E*; max. noncoupled respiration	0	low	Optimal external uncoupler concentration for max. oxygen flux	$J_{O2,k}$ by ET-capacity
ROX	*Rox*; min. residual O_2 consumption	0	0	$J_{O2,Rox}$ in non-ET-pathway oxidation reactions	Full inhibition of ET-pathway or absence of fuel substrates

394
395

LEAK-state (**Fig. 3**): The LEAK-state is defined as a state of mitochondrial respiration when O_2 flux mainly compensates for the proton leak in the absence of ATP synthesis, at kinetically-saturating concentrations of O_2 and respiratory substrates. LEAK-respiration is measured to obtain an indirect estimate of *intrinsic uncoupling* without addition of any experimental uncoupler: (*1*) in the absence of adenylates; (*2*) after depletion of ADP at maximum ATP/ADP ratio; or (*3*) after inhibition of the phosphorylation-pathway by inhibitors of ATP synthase, such as oligomycin, or adenine nucleotide translocase, such as carboxyatractyloside.

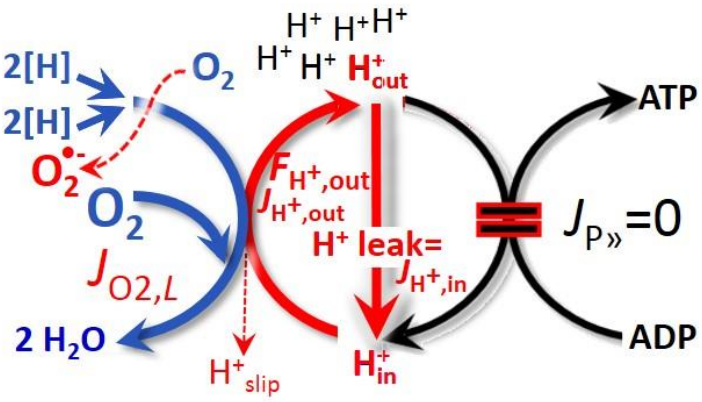

Fig. 3. LEAK-state: Phosphorylation is arrested, $J_{P»} = 0$, and oxygen flux, $J_{O2,L}$, is controlled mainly by the proton leak, which equals $J_{H+,in}$, at maximum protonmotive force, $F_{H+,out}$ (See also Fig. 2).

Table 2. Distinction of terms related to coupling.

Term	Respiration	P»/O_2	Note
Fully coupled	*P* – *L*	max.	OXPHOS-capacity corrected for LEAK-respiration (**Fig. 6**)
Well-coupled	*P*	High	Phosphorylating respiration with a variable intrinsic LEAK component (**Fig. 4**)
Loosely coupled	up to *E*	Low	Inducibly uncoupled by UCP1 or Ca^{2+} cycling
Dyscoupled	*P*	Low	Pathologically, toxicologically, environmentally increased uncoupling, mitochondrial dysfunction
Uncoupled and decoupled	*L*	0	Non-phosphorylating intrinsic LEAK-respiration without added protonophore (**Fig. 3**)
Noncoupled	*E*	0	Non-phosphorylating respiration stimulated to maximum flux at optimum exogenous uncoupler concentration (**Fig. 5**)

Proton leak: Proton leak is the *uncoupled* process in which protons are translocated across the mtIM in the dissipative direction of the downhill protonmotive force without coupling to phosphorylation (**Fig. 3**). The proton leak flux depends on the protonmotive force, is a property of the mtIM, may be enhanced due to possible contaminations by free fatty acids, and is physiologically controlled. In particular, inducible uncoupling mediated by uncoupling protein 1 (UCP1) is physiologically controlled, *e.g.*, in brown adipose tissue. UCP1 is a proton channel of the mtIM facilitating the conductance of protons across the mtIM (Klingenberg 2017). As a consequence of this effective short-circuit, the protonmotive force diminishes, resulting in stimulation of electron transfer to oxygen and heat dissipation without phosphorylation of ADP. Mitochondrial injuries may lead to *dyscoupling* as a pathological or toxicological cause of *uncoupled* respiration, *e.g.*, as a consequence of opening the permeability transition pore. Dyscoupled respiration is distinguished from the experimentally induced *noncoupled* respiration in the ET-state. Under physiological conditions, the proton leak is the dominant contributor to the overall leak current (Dufour *et al.* 1996).

Proton slip: Proton slip is the *decoupled* process in which protons are only partially translocated by a proton pump of the ET-pathways and slip back to the original compartment (Dufour *et al.* 1996). Proton slip can also happen in association with the ATP-synthase, in which case the proton slips downhill across the membrane to the matrix without contributing to ATP synthesis. In each case, proton slip is a property of the proton pump and increases with the turnover rate of the pump.

Cation cycling: Proton leak is a leak current of protons. There can be other cation contributors to leak current including calcium and probably magnesium. Calcium current is balanced by mitochondrial Na/Ca exchange, which is balanced by Na/H exchange or K/H exchange. This is another effective uncoupling mechanism different from proton leak and slip.

Small differences of terms, *e.g.*, uncoupled, noncoupled, are easily overlooked and may be erroneously perceived as identical. Even with an attempt at rigorous definition, the common use of such terms may remain vague (**Table 2**).

OXPHOS-state (**Fig. 4**): The OXPHOS-state is defined as the respiratory state with kinetically-saturating concentrations of O_2, respiratory and phosphorylation substrates, and absence of exogenous uncoupler, which provides an estimate of the maximal respiratory capacity in the OXPHOS-state for any given ET-pathway state. Respiratory capacities at kinetically-saturating substrate concentrations provide reference values or upper limits of performance, aiming at the generation of data sets for comparative purposes. Any effects of substrate kinetics are thus separated from reporting actual mitochondrial capacity for oxidation during well-coupled respiration, against which physiological activities can be evaluated.

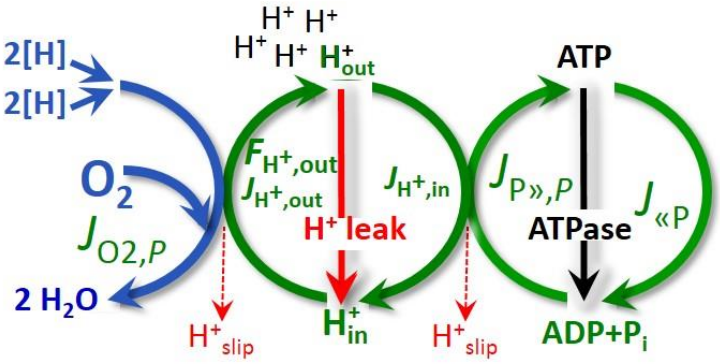

Fig. 4. OXPHOS-state: Phosphorylation, $J_{P»}$, is stimulated by kinetically-saturating [ADP] and inorganic phosphate, [P_i], and is supported by a high protonmotive force, $F_{H+,out}$. O_2 flux, $J_{O2,P}$, is well-coupled at a P»/O_2 ratio of $J_{P»,P}/J_{O2,P}$ (See also Fig. 2).

As discussed previously, 0.2 mM ADP does not fully saturate flux in isolated mitochondria (Gnaiger 2001; Puchowicz *et al.* 2004); greater ADP concentration is required, particularly in permeabilized muscle fibres and cardiomyocytes, to overcome limitations by intracellular diffusion and by the reduced conductance of the mitochondrial outer membrane, mtOM (Jepihhina *et al.* 2011, Illaste *et al.* 2012, Simson *et al*. 2016) either through interaction with tubulin (Rostovtseva *et al.* 2008) or other intracellular structures (Birkedal *et al*. 2014). In permeabilized muscle fibre bundles of high respiratory capacity, the apparent K_m for ADP increases up to 0.5 mM (Saks *et al.* 1998), indicating that >90% saturation is reached only at

463 >5 mM ADP. Similar ADP concentrations are also required for accurate determination of
464 OXPHOS-capacity in human clinical cancer samples and permeabilized cells (Klepinin *et al.*
465 2016; Koit *et al.* 2017). Whereas 2.5 to 5 mM ADP is sufficient to obtain the actual OXPHOS-
466 capacity in many types of permeabilized cell and tissue preparations, experimental validation
467 is required in each specific case.

468 **Electron transfer-state**
469 (**Fig. 5**): The ET-state is defined
470 as the *noncoupled* state with
471 kinetically-saturating
472 concentrations of O_2, respiratory
473 substrate and optimum
474 *exogenous* uncoupler
475 concentration for maximum O_2
476 flux, as an estimate of oxidative

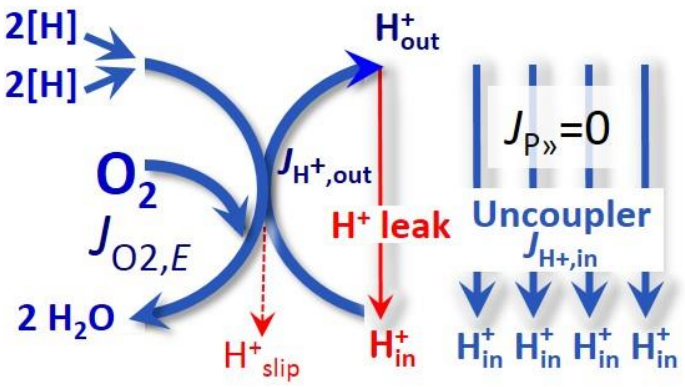

Fig. 5. ET-state: Noncoupled respiration, $J_{O2,E}$, is maximum at optimum exogenous uncoupler concentration and phosphorylation is zero, $J_{P»} = 0$ (See also Fig. 2).

477 ET-capacity. Inhibition of respiration is observed at higher than optimum uncoupler
478 concentrations. As a consequence of the nearly collapsed protonmotive force, the driving force
479 is insufficient for phosphorylation and $J_{P»} = 0$.

480 Besides the three fundamental coupling states of mitochondrial preparations, the
481 following respiratory state also is relevant to assess respiratory function:

482 **ROX:** Residual oxygen consumption (ROX) is defined as O_2 consumption due to
483 oxidative side reactions remaining after inhibition of ET with rotenone, malonic acid and
484 antimycin A. Cyanide and azide not only inhibit CIV but several peroxidases which might be
485 involved in ROX. ROX is not a coupling state but represents a baseline that is used to correct
486 mitochondrial respiration in defined coupling states. ROX is not necessarily equivalent to non-
487 mitochondrial respiration, considering oxygen-consuming reactions in mitochondria not related
488 to ET, such as oxygen consumption in reactions catalyzed by monoamine oxidases (type A and

B), monooxygenases (cytochrome P450 monooxygenases), dioxygenase (sulfur dioxygenase and trimethyllysine dioxygenase), several hydoxylases, and more. Mitochondrial preparations, especially those obtained from liver, are contaminated by peroxisomes. This fact makes the exact determination of mitochondrial oxygen consumption and mitochondria-associated generation of reactive oxygen species complicated (Schönfeld *et al.* 2009). The dependence of ROX-linked oxygen consumption needs to be studied in detail with respect to non-ET enzyme activities, availability of specific substrates, oxygen concentration, and electron leakage leading to the formation of reactive oxygen species.

2.2. Coupling states and respiratory rates

It is important to distinguish metabolic pathways from metabolic states and the corresponding metabolic rates; for example: ET-pathways (**Fig. 6**), ET-state (**Fig. 5**), and ET-capacity, *E*, respectively (**Table 1**). The protonmotive force is *high* in the OXPHOS-state when it drives phosphorylation, *maximum* in the LEAK-state of coupled mitochondria, driven by LEAK-respiration at a minimum back flux of protons to the matrix side, and *very low* in the ET-state when uncouplers short-circuit the proton cycle (**Table 1**).

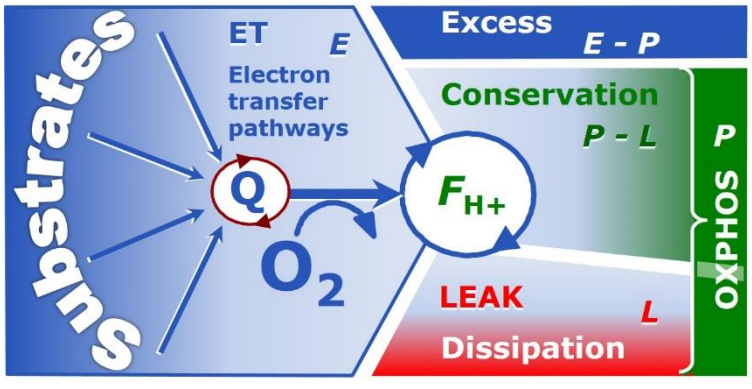

Fig. 6. Four-compartment model of oxidative phosphorylation. Respiratory states (ET, OXPHOS, LEAK) and corresponding rates (*E, P, L*) are connected by the protonmotive force, $F_{H+,out}$. Electron transfer-capacity, *E*, is partitioned into (*1*) dissipative LEAK-respiration, *L*, when the capacity to perform work is irreversibly lost, (*2*) net OXPHOS-capacity, *P-L*, with partial conservation of the capacity to perform work, and (*3*) the excess capacity, *E-P*. Modified from Gnaiger (2014).

The three coupling states, ET, LEAK and OXPHOS, are presented in a schematic context with the corresponding respiratory rates, abbreviated as *E*, *L* and *P*, respectively (**Fig. 6**). This clarifies that *E* may exceed or be equal to *P*, but *E* cannot theoretically be lower than *P*. *E* < *P* must be discounted as an artefact, which may be caused experimentally by: (*1*) loss of oxidative capacity during the time course of the respirometric assay, since *E* is measured subsequently to *P*; (*2*) using insuffient uncoupler concentrations; (*3*) using high uncoupler concentrations which inhibit ET (Gnaiger 2008); (*4*) high oligomycin concentrations applied for measurement of *L* before titrations of uncoupler, when oligomycin exerts an inhibitory effect on *E*. On the other hand, the excess ET-capacity is overestimated if non-saturating [P_i] or [ADP] are used (see State 3 in the next section).

E > *P* is observed in many types of mitochondria, varying between species, tissues and cell types. It is the excess ET-capacity pushing the phosphorylation-flux (**Fig. 1B**) to the limit of its *capacity of utilizing* the protonmotive force. Within any type of mitochondria, the magnitude of *E* > *P* depends on (*1*) the pathway control state with single or multiple electron input into the Q-junction and involvement of three or fewer coupling sites determining the H^+_{out}/O_2 *coupling stoichiometry* (**Fig. 1A**); and (*2*) the *biochemical coupling efficiency* expressed as *(E-L)/E*, since an increase of *L* causes *P* to increase towards the limit of *E*. The *excess E-P* capacity, *E-P*, therefore, provides a sensitive diagnostic indicator of specific injuries of the phosphorylation-pathway, under conditions when *E* remains constant but *P* declines relative to controls (**Fig. 6**). Substrate cocktails supporting simultaneous convergent electron transfer to the Q-junction for reconstitution of tricarboxylic acid cycle (TCA cycle) function establish pathway control states with high ET-capacity, and consequently increase the sensitivity of the *E-P* assay.

When subtracting *L* from *P*, the dissipative LEAK component in the OXPHOS-state may be overestimated. This can be avoided by measuring LEAK-respiration in a state when the protonmotive force is adjusted to its slightly lower value in the OXPHOS-state, *e.g.*, by titration

of an ET inhibitor. Any turnover-dependent components of proton leak and slip, however, are underestimated under these conditions (Garlid *et al.* 1993). In general, it is inappropriate to use the term *ATP production* or *ATP turnover* for the difference of oxygen consumption measured in states *P* and *L*. The difference *P-L* is the upper limit of the part of OXPHOS-capacity that is freely available for ATP production (corrected for LEAK-respiration) and is fully coupled to phosphorylation with a maximum mechanistic stoichiometry (**Fig. 6**).

2.3. Classical terminology for isolated mitochondria

> *'When a code is familiar enough, it ceases appearing like a code; one forgets that there is a decoding mechanism. The message is identical with its meaning'* (Hofstadter 1979).

Chance and Williams (1955; 1956) introduced five classical states of mitochondrial respiration and cytochrome redox states. **Table 3** shows a protocol with isolated mitochondria in a closed respirometric chamber, defining a sequence of respiratory states.

Table 3. Metabolic states of mitochondria (Chance and Williams, 1956; Table V).

State	$[O_2]$	ADP level	Substrate level	Respiration rate	Rate-limiting substance
1	>0	low	low	slow	ADP
2	>0	high	~0	slow	substrate
3	>0	high	high	fast	respiratory chain
4	>0	low	high	slow	ADP
5	0	high	high	0	oxygen

State 1 is obtained after addition of isolated mitochondria to air-saturated isoosmotic/isotonic respiration medium containing inorganic phosphate, but no fuel substrates and no adenylates, *i.e.*, AMP, ADP, ATP.

State 2 is induced by addition of a high concentration of ADP (typically 100 to 300 µM), which stimulates respiration transiently on the basis of endogenous fuel substrates and

phosphorylates only a small portion of the added ADP. State 2 is then obtained at a low respiratory activity limited by zero endogenous fuel substrate availability (**Table 3**). If addition of specific inhibitors of respiratory complexes, such as rotenone, does not cause a further decline of oxygen consumption, State 2 is equivalent to residual oxygen consumption (See below). If inhibition is observed, undefined endogenous fuel substrates are a confounding factor of pathway control by externally added substrates and inhibitors. In contrast to the original protocol, an alternative sequence of titration steps is frequently applied, in which the alternative State 2 has an entirely different meaning, when this second state is induced by addition of fuel substrate without ADP (LEAK-state; in contrast to State 2 defined in **Table 2** as a ROX state), followed by addition of ADP.

State 3 is the state stimulated by addition of fuel substrates while the ADP concentration is still high (**Table 3**) and supports coupled energy transformation through oxidative phosphorylation. 'High ADP' is a concentration of ADP specifically selected to allow the measurement of State 3 to State 4 transitions of isolated mitochondria in a closed respirometric chamber. Repeated ADP titration re-establishes State 3 at ‘high ADP’. Starting at oxygen concentrations near air-saturation (ca. 200 µM O_2 at sea level and 37 °C), the total ADP concentration added must be low enough (typically 100 to 300 µM) to allow phosphorylation to ATP at a coupled oxygen consumption that does not lead to oxygen depletion during the transition to State 4. In contrast, kinetically-saturating ADP concentrations usually are an order of magnitude higher than 'high ADP', *e.g.* 2.5 mM in isolated mitochondria. The abbreviation State 3u is frequently used in bioenergetics, to indicate the state of respiration after titration of an uncoupler, without sufficient emphasis on the fundamental difference between OXPHOS-capacity (*well-coupled* with an *endogenous* uncoupled component) and ET-capacity (*noncoupled*).

State 4 is a LEAK-state that is obtained only if the mitochondrial preparation is intact and well-coupled. Depletion of ADP by phosphorylation to ATP leads to a decline in oxygen

consumption in the transition from State 3 to State 4. Under these conditions, a maximum protonmotive force and high ATP/ADP ratio are maintained, and the P»/O_2 ratio can be calculated. State 4 respiration, L_T (**Table 1**), reflects intrinsic proton leak and intrinsic ATP hydrolysis activity. Oxygen consumption in State 4 is an overestimation of LEAK-respiration if the contaminating ATP hydrolysis activity recycles some ATP to ADP, $J_{«P}$, which stimulates respiration coupled to phosphorylation, $J_{P»} > 0$. This can be tested by inhibition of the phosphorylation-pathway using oligomycin, ensuring that $J_{P»} = 0$ (State 4o). Alternatively, sequential ADP titrations re-establish State 3, followed by State 3 to State 4 transitions while sufficient oxygen is available. However, anoxia may be reached before exhaustion of ADP (State 5).

State 5 is the state after exhaustion of oxygen in a closed respirometric chamber. Diffusion of oxygen from the surroundings into the aqueous solution may be a confounding factor preventing complete anoxia (Gnaiger 2001). Chance and Williams (1955) provide an alternative definition of State 5, which gives it the meaning of ROX: 'State 5 may be obtained by antimycin A treatment or by anaerobiosis'.

In **Table 3**, only States 3 and 4 (and 'State 2' in the alternative protocol without ADP; not included in the table) are coupling control states, with the restriction that O_2 flux in State 3 may be limited kinetically by non-saturating ADP concentrations (**Table 1**).

3. The protonmotive force and proton flux

3.1. Electric and chemical partial forces versus electrical and chemical units

The protonmotive force across the mtIM (Mitchell and Moyle 1967) was introduced most beautifully in the *Grey Book 1966* (see Mitchell 2011),

$$\Delta p_{H+} = \Delta\Psi + \Delta\mu_{H+}/F \qquad \text{(Eq. 1)}$$

The protonmotive force consists of two partial forces: (*1*) The electrical part, $\Delta\Psi$, is the difference of charge (electric potential difference), is not specific for H^+, and can, therefore, be

618 measured by the distribution of other cations between the positive and negative compartment
619 (**Fig. 2**). (*2*) The chemical part, $\Delta\mu_{H+}$, is the chemical potential difference in H^+, is proportional
620 to the pH difference, and incorporates the Faraday constant (**Table 4**).

621

622 **Table 4. Protonmotive force and flux matrix.** Columns: The protonmotive force is
623 the sum of *partial isomorphic forces*, F_{el} and $F_{H+,d}$. Rows: Electrical and chemical units
624 (isomorphic format *e* and *n*). The Faraday constant, *F*, converts protonmotive force
625 and flux from *format e* to *n*. In contrast to force (state), the conjugated flux (rate) cannot
626 be partitioned.
627

State		**Force**		**electric**	+	**chem.**	**Unit**	**Notes**
	Protonmotive force, *e*	Δp_{H+}	=	$\Delta\Psi$	+	$\Delta\mu_{H+}/F$	$J{\cdot}C^{-1}$	1*e*
	Chemiosmotic potential, *n*	$\Delta\tilde{\mu}_{H+}$	=	$\Delta\Psi{\cdot}F$	+	$\Delta\mu_{H+}$	$J{\cdot}mol^{-1}$	1*n*
State	**Isomorphic force**	$F_{H+,out/i}$		**el_{out}**	+	**$H^+_{out,d}$**		
	Electric charge, *e*	$F_{H+,out/e}$	=	$F_{el,out/e}$	+	$F_{H+,out,d/e}$	$J{\cdot}C^{-1}$	2*e*
	Amount of substance, *n*	$F_{H+,out/n}$	=	$F_{el,out/n}$	+	$F_{H+,out,d/n}$	$J{\cdot}mol^{-1}$	2*n*
Rate	**Isomorphic flux**	$J_{H+,out/i}$		***e***	**or**	***n***		
	Electric charge, *e*	$J_{H+,out/e}$		$J_{H+,out/e}$			$C{\cdot}s^{-1}{\cdot}m^{-3}$	3*e*
	Amount of substance, *n*	$J_{H+,out/n}$				$J_{H+,out/n}$	$mol{\cdot}s^{-1}{\cdot}m^{-3}$	3*n*

628

629 1: The Faraday constant, *F*, is the product of elementary charge (e = $1.602177{\cdot}10^{-19}{\cdot}$C) and the
630 Avogadro (Loschmidt) constant (N_A = $6.022136{\cdot}10^{23}{\cdot}mol^{-1}$), $F = eN_A$ = 96,485.3 C/mol. $\Delta\tilde{\mu}_{H+}$ is the
631 chemiosmotic potential difference. 1*e* and 1*n* are the classical representations of 2*e* and 2*n*.
632 2: The protonmotive force is $F_{H+,out}$, expressed either in isomorphic format *e* or *n*. $F_{el/e} \equiv \Delta\Psi$ is the partial
633 protonmotive force (el) acting generally on charged motive molecules (*i.e.* ions that are displaceable
634 across the mtIM). In contrast, $F_{H+,d/n} \equiv \Delta\mu_{H+}$ is the partial protonmotive force specific for proton
635 displacement (H^+_d). The sign of the force is negative for exergonic transformations in which exergy
636 is lost or dissipated, and positive for endergonic transformations which conserve exergy from a
637 coupled exergonic process (**Box 3**).
638 3: The sign of the flux depends on the definition of the compartmental direction of the translocation (**Fig.**
639 **2**). Flux x force = $J_{H+,out/e}{\cdot}F_{H+,out/e} = J_{H+,out/n}{\cdot}F_{H+,out/n}$ = volume-specific power [$J{\cdot}s^{-1}{\cdot}m^{-3} = W{\cdot}m^{-3}$].

Faraday constant, $F = eN_A$ [C/mol] (**Table 4**), enables the conversion between protonmotive force, $F_{H+,out/e} \equiv \Delta p_{H+}$ [J/C], expressed per *motive charge*, *e* [C], and protonmotive force or electrochemical potential difference, $F_{H+,out/n} \equiv \Delta\tilde{\mu}_{H+} = \Delta p_{H+} \cdot F$ [J/mol], expressed per *motive amount of protons*, *n* [mol]. Proton charge, *e*, and amount of substance, *n*, define the units for the isomorphic formats. Taken together, *F* converts protonmotive force and flux from isomorphic format *e* to *n* (Eq. 2; see also **Table 4**, Note 2),

$$F_{H+,out/n} = F_{H+,out/e} \cdot eN_A \quad \text{(Eq. 2.1)}$$

$$J_{H+,out/n} = J_{H+,out/e} / (eN_A) \quad \text{(Eq. 2.2)}$$

In each format, the protonmotive force is expressed as the sum of two partial forces. The concept expressed by the complex symbols in Eq. 1 can be explained and visualized more easily by *partial isomorphic forces* as the components of the protonmotive force:

Electrical part of the protonmotive force: (*1*) Isomorph *e:* $F_{el/e} \equiv \Delta\Psi$ is the electrical part of the protonmotive force expressed in units joule per coulomb, *i.e.* volt [V = J/C]. $F_{el/e}$ is defined as partial Gibbs energy change per *motive elementary charge*, *e* [C], not specific for proton charge (**Table 4**, Note 2*e*). (*2*) Isomorph *n:* $F_{el/n} \equiv \Delta\Psi \cdot F$ is the electric force expressed in units joule per mole [J/mol], defined as partial Gibbs energy change per *motive amount of charge*, *n* [mol], not specific for proton charge (**Table 4**, Note 2*n*).

Chemical part of the protonmotive force: (*1*) Isomorph *n:* $F_{d,H+/n} \equiv \Delta\mu_{H+}$ is the chemical part (diffusion, displacement of H^+) of the protonmotive force expressed in units joule per mole [J/mol]. $F_{d,H+/n}$ is defined as partial Gibbs energy change per *motive amount of protons*, *n* [mol] (**Table 4**, Note 2*n*). (*2*) Isomorph *e*: $F_{d,H+/e} \equiv \Delta\mu_{H+}/F$ is the chemical force expressed in units joule per coulomb [V], defined as partial Gibbs energy change per *motive amount of protons expressed in units of electric charge, e* [C], but specific for proton charge (**Table 4**, Note 2*e*).

Protonmotive means that there is a potential for the movement of protons, and force is a measure of the potential for motion. Motion is relative and not absolute (Principle of Galilean

Relativity); likewise there is no absolute potential, but (isomorphic) forces are potential differences. An electric partial force expressed in the format of electric charge, $F_{el/e}$, of -0.2 V (**Table 5**, Note 5*e*) is equivalent to force in the format of amount, $F_{el,H+/n}$, of 19 kJ·mol^{-1} H^+_{out} (Note 5*n*). For a ΔpH of 1 unit, the chemical partial force in the format of amount, $F_{d,H+/n}$, changes by 5.9 kJ·mol^{-1} (**Table 5**, Note 6*n*) and chemical force in the format of charge $F_{d,H+/e}$ changes by 0.06 V (Note 6*e*). Considering a driving force of -470 kJ·mol^{-1} O_2 for oxidation, the thermodynamic limit of the H^+_{out}/O_2 ratio is reached at a value of 470/19 = 24, compared to a mechanistic stoichiometry of 20 (**Fig. 1**).

3.2. Definitions

Control and regulation: The terms metabolic *control* and *regulation* are frequently used synonymously, but are distinguished in metabolic control analysis: 'We could understand the regulation as the mechanism that occurs when a system maintains some variable constant over time, in spite of fluctuations in external conditions (homeostasis of the internal state). On the other hand, metabolic control is the power to change the state of the metabolism in response to an external signal' (Fell 1997). Respiratory control may be induced by experimental control signals that *exert* an influence on: (*1*) ATP demand and ADP phosphorylation-rate; (*2*) fuel substrate composition, pathway competition; (*3*) available amounts of substrates and oxygen, *e.g.*, starvation and hypoxia; (*3*) the protonmotive force, redox states, flux-force relationships, coupling and efficiency; (*4*) Ca^{2+} and other ions including H^+; (*5*) inhibitors, *e.g.*, nitric oxide or intermediary metabolites, such as oxaloacetate; (*6*) signalling pathways and regulatory proteins, *e.g.* insulin resistance, transcription factor HIF-1 or inhibitory factor 1. *Mechanisms* of respiratory control and regulation include adjustments of (*1*) enzyme activities by allosteric mechanisms and phosphorylation, (*2*) enzyme content, concentrations of cofactors and conserved moieties (such as adenylates, nicotinamide adenine dinucleotide [NAD^+/NADH], coenzyme Q, cytochrome *c*); (*3*) metabolic channeling by supercomplexes; and *(4)*

692 mitochondrial density (enzyme concentrations and membrane area) and morphology (cristae
693 folding, fission and fusion). (*5*) Mitochondria are targeted directly by hormones, thereby
694 affecting their energy metabolism (Lee *et al.* 2013; Gerö and Szabo 2016; Price and Dai 2016;
695 Moreno *et al.* 2017). Evolutionary or acquired differences in the genetic and epigenetic basis
696 of mitochondrial function (or dysfunction) between subjects and gene therapy; age; gender,
697 biological sex, and hormone concentrations; life style including exercise and nutrition; and
698 environmental issues including thermal, atmospheric, toxicological and pharmacological
699 factors, exert an influence on all control mechanisms listed above (for reviews, see Brown 1992;
700 Gnaiger 1993a, 2009; 2014; Paradies *et al.* 2014; Morrow *et al*. 2017).

701 **Respiratory control and response:** Lack of control by a metabolic pathway, *e.g.*
702 phosphorylation-pathway, does mean that there will be no response to a variable activating it,
703 *e.g.* [ADP]. However, the reverse is not true as the absence of a response to [ADP] does not
704 exclude the phosphorylation-pathway from having some degree of control. The degree of
705 control of a component of the OXPHOS-pathway on an output variable, such as oxygen flux,
706 will in general be different from the degree of control on other outputs, such as phosphorylation-
707 flux or proton leak flux (**Box 2**). As such, it is necessary to be specific as to which input and
708 output are under consideration (Fell 1997). Therefore, the term respiratory control is elaborated
709 in more detail in the following section.

710 **Respiratory coupling control:** Respiratory control refers to the ability of mitochondria
711 to adjust oxygen consumption in response to external control signals by engaging various
712 mechanisms of control and regulation. Respiratory control is monitored in a mitochondrial
713 preparation under conditions defined as respiratory states. When phosphorylation of ADP to
714 ATP is stimulated or depressed, an increase or decrease is observed in electron flux linked to
715 oxygen consumption in respiratory coupling states of intact mitochondria (‘controlled states’ in
716 the classical terminology of bioenergetics). Alternatively, coupling of electron transfer with
717 phosphorylation is disengaged by disruption of the integrity of the mtIM or by uncouplers,

functioning like a clutch in a mechanical system. The corresponding coupling control state is characterized by high levels of oxygen consumption without control by phosphorylation ('uncontrolled state'). Energetic coupling is defined in **Box 4**. Loss of coupling lowers the efficiency by intrinsic uncoupling and decoupling, or pathological dyscoupling. Such generalized uncoupling is different from switching to mitochondrial pathways that involve fewer than three proton pumps ('coupling sites': Complexes CI, CIII and CIV), bypassing CI through multiple electron entries into the Q-junction (**Fig. 1**). A bypass of CIII and CIV is provided by alternative oxidases, which reduce oxygen without proton translocation. Reprogramming of mitochondrial pathways may be considered as a switch of gears (changing the stoichiometry) rather than uncoupling (loosening the stoichiometry).

Pathway control states are obtained in mitochondrial preparations by depletion of endogenous substrates and addition to the mitochondrial respiration medium of fuel substrates (CHNO) and specific inhibitors, activating selected mitochondrial pathways (**Fig. 1**). Coupling control states and pathway control states are complementary, since mitochondrial preparations depend on an exogenous supply of pathway-specific fuel substrates and oxygen (Gnaiger 2014).

Box 2: Metabolic fluxes and flows: vectorial and scalar

In mitochondrial electron transfer (**Fig. 1**), vectorial transmembrane proton flux is coupled through the proton pumps CI, CIII and CIV to the catabolic flux of scalar reactions, collectively measured as oxygen flux. In **Fig. 2**, the scalar catabolic reaction, k, of oxygen consumption, $J_{O2,k}$ [mol·s^{-1}·m^{-3}], is expressed as oxygen flux per volume, V [m^3], of the instrumental chamber (the system).

Fluxes are *vectors*, if they have *spatial* direction in addition to magnitude. A vector flux (surface-density of flow) is expressed per unit cross-sectional area, A [m^2], perpendicular to the direction of flux. If *flows*, I, are defined as extensive quantities of the *system*, as vector or scalar flow, $\boldsymbol{I}$ or I [mol·s^{-1}], respectively, then the corresponding vector and scalar *fluxes*, J, are

obtained as $\boldsymbol{J} = \boldsymbol{I} \cdot A^{-1}$ [mol·s^{-1}·m^{-2}] and $J = I \cdot V^{-1}$ [mol·s^{-1}·m^{-3}], respectively, expressing flux as an area-specific vector or volume-specific scalar quantity.

Vectorial transmembrane proton flux, $J_{H+,out}$, is analyzed in a heterogenous compartmental system as a quantity with *directional* but not *spatial* information. Translocation of protons across the mtIM has a defined direction, either from the negative compartment (matrix space; negative or $^{-}$Compartment) to the positive compartment (inter-membrane space; positive or $^{+}$Compartment) or *vice versa* (**Fig. 2**). The arrows defining the direction of the translocation between the two compartments may point upwards or downwards, right or left, without any implication that these are actual directions in space. The 'upper' compartment of the $^{+}$Compartment is neither above nor below the $^{-}$Compartment in a spatial sense, but can be visualized arbitrarily in a figure as the upper compartment (**Fig. 2**). In general, the *compartmental direction* of vectorial translocation from the $^{-}$Compartment to the $^{+}$Compartment is defined by assigning the initial and final state as *ergodynamic compartments*, $H^{+}_{in} \rightarrow H^{+}_{out}$, respectively, related to work (erg = work) that must be performed to lift the proton from a lower to a higher electrochemical potential or from the lower to the higher ergodynamic compartment (Gnaiger 1993b).

In direct analogy to *vectorial* translocation, the direction of a *scalar* chemical reaction, A → B, is defined by assigning substrates and products, A and B, as ergodynamic compartments. O_2 is defined as a substrate in respiratory O_2 consumption, which together with the fuel substrates comprises the substrate compartment of the catabolic reaction (**Fig. 2**). Volume-specific scalar O_2 flux is coupled (**Box 4**) to vectorial translocation. In order to establish a quantitative relation between the coupled fluxes, both $J_{O2,k}$ and $J_{H+,out}$ must be expressed in identical isomorphic units ([mol·s^{-1}·m^{-3}] or [C·s^{-1}·m^{-3}]), yielding the H^{+}_{out}/O_2 ratio (**Fig. 1**). The *vectorial* proton flux in compartmental translocation has *compartmental direction*, distinguished from a *vector* flux with *spatial direction*. Likewise, the corresponding protonmotive force is defined as an electrochemical potential *difference* between two

compartments, in contrast to a *gradient* across the membrane or a vector force with defined spatial direction.

The steady-state: Mitochondria represent a thermodynamically open system functioning as a biochemical transformation system in non-equilibrium states. State variables (protonmotive force; redox states) and metabolic fluxes (*rates*) are measured in defined mitochondrial respiratory *states*. Strictly, steady states can be obtained only in open systems, in which changes due to *internal* transformations, *e.g.*, O_2 consumption, are instantaneously compensated for by *external* fluxes *e.g.*, O_2 supply, such that oxygen concentration does not change in the system (Gnaiger 1993b). Mitochondrial respiratory states monitored in closed systems satisfy the criteria of pseudo-steady states for limited periods of time, when changes in the system (concentrations of O_2, fuel substrates, ADP, P_i, H^+) do not exert significant effects on metabolic fluxes (respiration, phosphorylation). Such pseudo-steady states require respiratory media with sufficient buffering capacity and kinetically-saturating concentrations of substrates to be maintained, and thus depend on the kinetics of the processes under investigation. Proton turnover, $J_{\infty H+}$, and ATP turnover, $J_{\infty P}$, proceed in the steady-state at constant $F_{H+,out}$, when $J_{\infty H+} = J_{H+,out} = J_{H+,in}$, and at constant $F_{P»}$, when $J_{\infty P} = J_{P»} = J_{«P}$ (**Fig. 2**).

Box 3: Endergonic and exergonic transformations, exergy and dissipation

A chemical reaction, or any transformation, is exergonic if the Gibbs energy change (exergy) of the reaction is negative at constant temperature and pressure. The sum of Gibbs energy changes of all internal transformations in a system can only be negative, *i.e.* exergy is irreversibly dissipated. Endergonic reactions are characterized by positive Gibbs energies of reaction and cannot proceed spontaneously in the forward direction as defined. For instance, the endergonic reaction P» is coupled to exergonic catabolic reactions, such that the total Gibbs energy change is negative, *i.e.* exergy must be dissipated for the reaction to proceed (**Fig. 2**).

In contrast, energy cannot be lost or produced in any internal process, which is the key message of the first law of thermodynamics. Thus mitochondria are the sites of energy transformation but not energy production. Open and closed systems can gain energy and exergy only by external fluxes, *i.e.* uptake from the environment. Exergy is the potential to perform work. In the framework of flux-force relationships (**Box 4**), the *partial* derivative of Gibbs energy per advancement of a transformation is an isomorphic force, F_{tr} (**Table 5**, Note 2). In other words, force is equal to exergy/motive unit (in integral form, this definition takes care of non-isothermal processes). This formal generalization represents an appreciation of the conceptual beauty of Peter Mitchell's innovation of the protonmotive force against the background of the established paradigm of the electromotive force (emf) defined at the limit of zero current (Cohen *et al.* 2008).

Table 5. Power, exergy, force, flux, and advancement.

Expression	Symbol	Definition	Unit	Notes
Power, volume-specific	$P_{V,tr}$	$P_{V,tr} = J_{tr} \cdot F_{tr} = \partial_{tr}G \cdot \partial t^{-1}$	$W = J \cdot s^{-1} \cdot m^{-3}$	1
Force, isomorphic	F_{tr}	$F_{tr} = \partial_{tr}G \cdot \partial_{tr}\xi^{-1}$	$J \cdot x^{-1}$	2
Flux, isomorphic	J_{tr}	$J_{tr} = d_{tr}\xi \cdot dt^{-1} \cdot V^{-1}$	$x \cdot s^{-1} \cdot m^{-3}$	3
Advancement, *n*	$d_{tr}\xi_{H+/n}$	$d_{tr}\xi_{H+/n} = d_{tr}n_{H+} \cdot \nu_{H+}^{-1}$	mol	4*n*
Advancement, *e*	$d_{tr}\xi_{H+/e}$	$d_{tr}\xi_{H+/e} = d_{tr}e_{H+} \cdot \nu_{H+}^{-1}$	C	4*e*
Electric partial force, *e*	$F_{el/e}$	$F_{el/e} \equiv \Delta\Psi$	V	5*e*
Electric partial force, *n*	$F_{el/n}$	$\Delta\Psi \cdot F = 96.5 \cdot \Delta\Psi$	$kJ \cdot mol^{-1}$	5*n*
Chemical partial force, *e*	$F_{d,H+/e}$	$\Delta\mu_{H+}/F = -\ln(10) \cdot RT/F \cdot \Delta pH$	V	6*e*
at 37 °C		$= -0.06 \cdot \Delta pH$	$J \cdot C^{-1}$	
Chemical partial force, *n*	$F_{d,H+/n}$	$\Delta\mu_{H+} = -\ln(10) \cdot RT \cdot \Delta pH$	$J \cdot mol^{-1}$	6*n*
at 37 °C		$= -5.9 \cdot \Delta pH$	$kJ \cdot mol^{-1}$	

1 to 4: An isomorphic motive entity or transformant, expressed in units x, is defined for any transformation, tr. x = mol or C in proton translocation.

2: $\partial_{tr}G$ [J] is the partial Gibbs energy change in the advancement of transformation tr.

3: For x = C, flow is electric current, I_{el} [A = C·s^{-1}], vector flux is electric current density per area, $\boldsymbol{J}_{el}$, and compartmental flux is electric current density per volume, I_{el} [A·m^{-3}].

4*n*: For a chemical reaction, the advancement of reaction r is $d_r\xi_B = d_r n_B \cdot \nu_B^{-1}$ [mol]. The stoichiometric number is $\nu_B = -1$ or $\nu_B = 1$, depending on B being a product or substrate, respectively, in reaction r involving one mole of B. The conjugated *intensive* molar quantity, $F_{B,r} = \partial_r G/\partial_r \xi_B$ [J·mol^{-1}], is the chemical force of reaction or *reaction-motive* force per stoichiometric amount of B. In reaction kinetics, $d_r n_B$ is expressed as a volume-specific quantity, which is the partial contribution to the total concentration change of B, $d_r c_B = d_r n_B/V$ and $dc_B = dn_B/V$, respectively. In open systems with constant volume V, $dc_B = d_r c_B + d_e c_B$, where r indicates the *internal* reaction and e indicates the *external* flux of B into the unit volume of the system. At steady state the concentration does not change, $dc_B = 0$, when $d_r c_B$ is compensated for by the external flux of B, $d_r c_B = -d_e c_B$ (Gnaiger 1993b). Alternatively, $dc_B = 0$ when B is held constant by different coupled reactions in which B acts as a substrate or a product.

4*e*: Scalar potential difference across the mitochondrial membrane. In a scalar electric transformation (flux of charge, *i.e.* volume-specific current, from the matrix space to the intermembrane and extramitochondrial space) the motive force is the difference of charge (**Box 2**). The endergonic direction of translocation is defined in **Fig. 2** as $H^+_{in} \rightarrow H^+_{out}$.

5*n*: F = 96.5 (kJ·mol^{-1})/V.

6: The electric partial force is independent of temperature (Note 5), but the chemical partial force depends on absolute temperature, T [K].

6*e*: RT is the gas constant times absolute temperature. ln(10)·RT/F = 59.16 and 61.54 mV at 298.15 and 310.15 K (25 and 37 °C), respectively.

6*n*: ln(10)·RT = 5.708 and 5.938 kJ·mol^{-1} at 298.15 and 310.15 K (25 and 37 °C), respectively.

3.3. Forces and fluxes in physics and irreversible thermodynamics

According to its definition in physics, a potential difference and as such the *protonmotive force*, Δp_{H+}, is not a force *per se* (Cohen *et al.* 2008). The fundamental forces of physics are distinguished from *motive forces* of statistical and irreversible thermodynamics. Complementary to the attempt towards unification of fundamental forces defined in physics,

844 the concepts of Nobel laureates Lars Onsager, Erwin Schrödinger, Ilya Prigogine and Peter
845 Mitchell (even if expressed in apparently unrelated terms) unite the diversity of *generalized* or
846 'isomorphic' *flux-force* relationships, the product of which links to the dissipation function and
847 Second Law of thermodynamics (Schrödinger 1944; Prigogine 1967). A *motive force* is the
848 derivative of potentially available or 'free' energy (exergy) per isomorphic *motive* unit (**Box 3**).
849 Perhaps the first account of a *motive force* in energy transformation can be traced back to the
850 Peripatetic school around 300 BC in the context of moving a lever, up to Newton's motive force
851 proportional to the alteration of motion (Coopersmith 2010).

852 **Vectorial and scalar forces, and fluxes:** In chemical reactions and osmotic or diffusion
853 processes occurring in a closed heterogeneous system, such as a chamber containing isolated
854 mitochondria, scalar transformations occur without measured spatial direction but between
855 separate compartments (translocation between the matrix and intermembrane space) or between
856 energetically-separated chemical substances (reactions from substrates to products). Hence, the
857 corresponding fluxes are not vectorial but scalar, and are expressed per volume and not per
858 membrane area (**Box 2**). The corresponding motive forces are also scalar potential *differences*
859 across the membrane (**Table 5**), without taking into account the *gradients* across the 6 nm thick
860 mtIM (Rich 2003).

861 **Coupling:** In energetics (ergodynamics), coupling is defined as an energy transformation
862 fuelled by an exergonic (downhill) input process driving the advancement of an endergonic
863 (uphill) output process. The (negative) output/input power ratio is the efficiency of a coupled
864 energy transformation (**Box 4**). At the limit of maximum efficiency of a completely coupled
865 system, the (negative) input power equals the (positive) output power, such that the total power
866 approaches zero at the maximum efficiency of 1, and the process becomes fully reversible
867 without any dissipation of exergy, *i.e.* without entropy production.

868

869

870

871 **Box 4: Coupling, power and efficiency, at constant temperature and pressure**

872 Energetic coupling means that two processes of energy transformation are linked such that the
873 input power, P_{in}, is the driving element of the output power, P_{out}, and the out/input power ratio
874 is the efficiency. In general, power is work per unit time [$J.s^{-1}$ = W]. When describing a system
875 with volume V without information on the internal structure, the output is defined as the *external*
876 work (exergy) performed by the *total* system on its environment. Such a system may be open
877 for any type of exchange, or closed and thus allowing only heat and work to be exchanged
878 across the system boundaries. This is the classical black box approach of thermodynamics. In
879 contrast, in a colourful compartmental analysis of *internal* energy transformations (**Fig. 2**), the
880 system is structured and described by definition of ergodynamic compartments (with
881 information on the heterogeneity of the system; **Box 2**) and analysis of separate parts, *i.e.* a
882 sequence of *partial* energy transformations, tr. In general, power per unit volume, P_{tr}/V [$W.L^{-1}$],
883 is the product of a volume-specific flux, J_{tr}, and its conjugated force, F_{tr}, and is closely linked
884 to the dissipation function using the terminology of irreversible thermodynamics (Prigogine
885 1967; Gnaiger 1993a,b). Output power of proton translocation and catabolic input power are
886 (**Fig. 2**),

887 Output: $P_{H+,out}/V = J_{H+,out} \cdot F_{H+,out}$

888 Input: $P_k/V = J_{O2,k} \cdot F_{O2,k}$

889 $F_{O2,k}$ is the exergonic input force with a negative sign, and, $F_{H+,out}$, is the endergonic output
890 force with a positive sign (**Box 3**). Ergodynamic efficiency is the ratio of output/input power,
891 or the flux ratio times force ratio (Gnaiger 1993a,b),

892 $$\varepsilon = \frac{P_{H+,out}}{-P_k} = \frac{J_{H+,out}}{J_{O2,k}} \cdot \frac{F_{H+,out}}{-F_{O2,k}}$$

893 The concept of incomplete coupling relates exclusively to the first term, *i.e.* the flux ratio, or
894 H^+_{out}/O_2 ratio (**Fig. 1**). Likewise, respirometric definitions of the P»/O_2 ratio and biochemical

coupling efficiency (Section 3.2) consider flux ratios. In a completely coupled process, the power efficiency, ε, depends entirely on the force ratio, ranging from zero efficiency at an output force of zero, to the limiting output force and maximum efficiency of 1.0, when the total power of the coupled process, $P_t = P_k + P_{H+,out}$, equals zero, and any net flows are zero at ergodynamic equilibrium of a coupled process. Thermodynamic equilibrium is defined as the state when all potentials (all forces) are dissipated and equilibrate towards their minima of zero. In a fully or completely coupled process, output and input fluxes are directly proportional in a fixed ratio technically defined as a stoichiometric relationship (a gear ratio in a mechanical system). Such maximal stoichiometric output/input flux ratios are considered in OXPHOS analysis as the upper limits or mechanistic H^+_{out}/O_2 and $P\gg/O_2$ ratios (**Fig. 1**).

Coupled versus bound processes: Since the chemiosmotic theory describes the mechanisms of coupling in OXPHOS, it may be interesting to ask if the electrical and chemical parts of proton translocation are coupled processes. This is not the case according to the definition of coupling. If the coupling mechanism is disengaged, the output process becomes independent of the input process, and both proceed in their downhill (exergonic) direction (**Fig. 2**). It is not possible to physically uncouple the electrical and chemical processes, which are only *theoretically* partitioned as electrical and chemical components and can be measured separately. If partial processes are non-separable, *i.e.*, cannot be uncoupled, then these are not *coupled* but are defined as *bound* processes. The electrical and chemical parts are tightly bound partial forces of the protonmotive force, since a flux cannot be partitioned but expressed only in either an electrical or chemical isomorphic format (**Table 4**).

4. Normalization: fluxes and flows

The challenges of measuring mitochondrial respiratory flux are matched by those of normalization, whereby O_2 consumption may be considered as the numerator and normalization

as the complementary denominator, which are tightly linked in reporting the measurements in a format commensurate with the requirements of a database.

4.1. Flux per chamber volume

When the reactor volume does not change during the reaction, which is typical for liquid phase reactions, the volume-specific *flux of a chemical reaction* r is the time derivative of the advancement of the reaction per unit volume, $J_{V,B} = d_r\xi_B/dt \cdot V^{-1}$ [(mol·s^{-1})·L^{-1}]. The *rate of concentration change* is dc_B/dt [(mol·L^{-1})·s^{-1}], where concentration is $c_B = n_B/V$. It is helpful to make the subtle distinction between [mol·s^{-1}·L^{-1}] and [mol·L^{-1}·s^{-1}] for the fundamentally different quantities of volume-specific flux and rate of concentration change, which merge to a single expression only in closed systems. In open systems, external fluxes (such as O_2 supply) are distinguished from internal transformations (metabolic flux, O_2 consumption). In a closed system, external flows of all substances are zero and O_2 consumption (internal flow), I_{O2} [pmol·s^{-1}], causes a decline of the amount of O_2 in the system, n_{O2} [nmol]. Normalization of these quantities for the volume of the system, V [L = dm^3], yields volume-specific O_2 flux, $J_{V,O2} = I_{O2}/V$ [nmol·s^{-1}·L^{-1}], and O_2 concentration, [O_2] or $c_{O2} = n_{O2}/V$ [nmol·mL^{-1} = µmol·L^{-1} = µM]. Instrumental background O_2 flux is due to external flux into a non-ideal closed respirometer, such that total volume-specific flux has to be corrected for instrumental background O_2 flux, *i.e.* O_2 diffusion into or out of the instrumental chamber. $J_{V,O2}$ is relevant mainly for methodological reasons and should be compared with the accuracy of instrumental resolution of background-corrected flux, *e.g.* ±1 nmol·s^{-1}·L^{-1} (Gnaiger 2001). 'Metabolic' or catabolic indicates O_2 flux, $J_{O2,k}$, corrected for instrumental background O_2 flux and chemical background O_2 flux due to autoxidation of chemical components added to the incubation medium.

947 *4.2. System-specific and sample-specific normalization*

948 Application of common and generally defined units is required for direct transfer of
949 reported results into a database. The second [s] is the *SI* unit for the base quantity *time*. It is also
950 the standard time-unit used in solution chemical kinetics. **Table 6** lists some conversion factors
951 to obtain *SI* units. The term *rate* is not sufficiently defined to be useful for a database (**Fig. 7**).
952 The inconsistency of the meanings of rate becomes fully apparent when considering Galileo
953 Galilei's famous principle, that 'bodies of different weight all fall at the same rate (have a
954 constant acceleration)' (Coopersmith 2010).

955 **Extensive quantities:** An extensive quantity increases proportionally with system size.
956 The magnitude of an extensive quantity is completely additive for non-interacting subsystems,
957 such as mass or flow expressed per defined system. The magnitude of these quantities depends
958 on the extent or size of the system (Cohen *et al.* 2008).

959

960 **Fig. 7. Different meanings of *rate* may lead to confusion, if the normalization is not sufficiently specified.** Results are frequently expressed as mass-specific *flux*, J_m, per mg protein, dry or wet weight (mass). Cell volume, V_{cell}, or mitochondrial volume, V_{mt}, may be used for normalization (volume-specific flux, J_{Vcell} or J_{Vmt}), which then must be clearly distinguished from flux, J_V, expressed for methodological reasons per volume of the measurement system, or flow per cell, I_X.

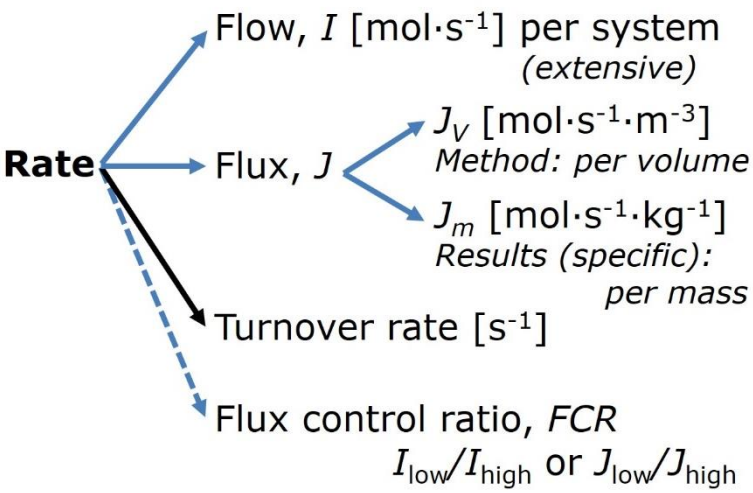

971

972 **Size-specific quantities:** 'The adjective *specific* before the name of an extensive quantity
973 is often used to mean *divided by mass*' (Cohen *et al.* 2008). Mass-specific flux is flow divided
974 by mass of the system. A mass-specific quantity is independent of the extent of non-interacting

homogenous subsystems. Tissue-specific quantities are of fundamental interest in comparative mitochondrial physiology, where *specific* refers to the *type* rather than *mass* of the tissue. The term *specific*, therefore, must be further clarified, such that tissue mass-specific, *e.g.*, muscle mass-specific quantities are defined.

Molar quantities: 'The adjective *molar* before the name of an extensive quantity generally means *divided by amount of substance*' (Cohen *et al.* 2008). The notion that all molar quantities then become *intensive* causes ambiguity in the meaning of *molar Gibbs energy*. It is important to emphasize the fundamental difference between normalization for amount of substance *in a system* or for amount of motive substance *in a transformation*. When the Gibbs energy of a system, G [J], is divided by the amount of substance B in the system, n_B [mol], a *size-specific* molar quantity is obtained, $G_B = G/n_B$ [J·mol^{-1}], which is not any force at all. In contrast, when the partial Gibbs energy change, $\partial_r G$ [J], is divided by the motive amount of substance B in reaction r (advancement of reaction), $\partial_r\xi_B$ [mol], the resulting intensive molar quantity, $F_{B,r} = \partial G/\partial_r\xi_B$ [J·mol^{-1}], is the chemical motive force of reaction r involving 1 mol B (**Table 5**, Note 4).

Flow per system, *I*: In analogy to electrical terms, flow as an extensive quantity (I; per system) is distinguished from flux as a size-specific quantity (J; per system size) (**Fig. 7**). Electric current is flow, I_{el} [A = C·s^{-1}] per system (extensive quantity). When dividing this extensive quantity by system size (membrane area), a size-specific quantity is obtained, which is electric flux (electric current density), $\boldsymbol{J}_{el}$ [A·m^{-2} = C·s^{-1}·m^{-2}].

Size-specific flux, *J*: Metabolic O_2 flow per tissue increases as tissue mass is increased. Tissue mass-specific O_2 flux should be independent of the size of the tissue sample studied in the instrument chamber, but volume-specific O_2 flux (per volume of the instrument chamber, V) should increase in direct proportion to the amount of sample in the chamber. Accurate definition of the experimental system is decisive: whether the experimental chamber is the closed, open, isothermal or non-isothermal *system* with defined volume as part of the

measurement apparatus, in contrast to the experimental *sample* in the chamber (**Table 6**). Volume-specific O_2 flux depends on mass-concentration of the sample in the chamber, but should be independent of the chamber volume. There are practical limitations to increasing the mass-concentration of the sample in the chamber, when one is concerned about crowding effects and instrumental time resolution.

Sample concentration C_{mX}: Normalization for sample concentration is required for reporting respiratory data. Consider a tissue or cells as the sample, X, and the sample mass, m_X [mg] from which a mitochondrial preparation is obtained. The sample mass, m_X, is frequently measured as wet or dry weight, W_w or W_d [mg], or as amount of tissue or cell protein, $m_{Protein}$. In the case of permeabilized tissues, cells, and homogenates, the sample concentration, $C_{mX} = m_X/V$ [mg·mL^{-1} = g·L^{-1}], is simply the mass of the subsample of tissue that is transferred into the instrument chamber. Part of the mitochondria from the tissue is lost during preparation of isolated mitochondria, and only a fraction of mitochondria is obtained, expressed as the mitochondrial yield (**Fig. 8**). At a high mitochondrial yield the sample of isolated mitochondria is more representative of the total mitochondrial population than in preparations characterized by low mitochondrial yield. Determination of the mitochondrial yield is based on measurement of the concentration of a mitochondrial marker in the tissue homogenate, $C_{mte,thom}$, which simultaneously provides information on the specific mitochondrial density in the sample (**Fig. 8**).

Tissues can contain multiple cell populations which may have distinct mitochondrial subtypes. Mitochondria are also in a constant state of flux due to highly dynamic fission and fusion cycles, and can exist in multiple stages and sizes which may be altered by a range of factors. The isolation of mitochondria (often achieved through differential centrifugation) can therefore yield a subsample of the mitochondrial types present in a tissue, dependent on isolation protocols utilized (*e.g.* centrifugation speed). This possible artefact should be taken into account when planning experiments using isolated mitochondria. The tendency for

mitochondria of specific sizes to be enriched at different centrifugation speeds also has the potential to allow the isolation of specific mitochondrial subpopulations and therefore the analysis of mitochondria from multiple cell lineages within a single tissue.

Table 6. Sample concentrations and normalization of flux with *SI* base units.

Expression	Symbol	Definition	*SI* Unit	Notes
Sample				
Identity of sample	X	Cells, animals, patients		
Number of sample entities X	N_X	Number of cells, *etc.*	x	
Mass of sample X	m_X		kg	1
Mass of entity X	M_X	$M_X = m_X \cdot N_X^{-1}$	$kg \cdot x^{-1}$	1
Mitochondria				
Mitochondria	mt	X = mt		
Amount of mt-elements	mte	Quantity of mt-marker	x_{mte}	
Concentrations				
Sample number concentration	C_{NX}	$C_{NX} = N_X \cdot V^{-1}$	$x \cdot m^{-3}$	2
Sample mass concentration	C_{mX}	$C_{mX} = m_X \cdot V^{-1}$	$kg \cdot m^{-3}$	
Mitochondrial concentration	C_{mte}	$C_{mte} = mte \cdot V^{-1}$	$x_{mte} \cdot m^{-3}$	3
Specific mitochondrial density	D_{mte}	$D_{mte} = mte \cdot m_X^{-1}$	$x_{mte} \cdot kg^{-1}$	4
Mitochondrial content, mte per entity X	mte_X	$mte_X = mte \cdot N_X^{-1}$	$x_{mte} \cdot x^{-1}$	5
O_2 flow and flux				6
Flow	I_{O2}	Internal flow	$mol \cdot s^{-1}$	7
Volume-specific flux	$J_{V,O2}$	$J_{V,O2} = I_{O2} \cdot V^{-1}$	$mol \cdot s^{-1} \cdot m^{-3}$	8
Flow per sample entity X	$I_{X,O2}$	$I_{X,O2} = J_{V,O2} \cdot C_{NX}^{-1}$	$mol \cdot s^{-1} \cdot x^{-1}$	9
Mass-specific flux	$J_{mX,O2}$	$J_{mX,O2} = J_{V,O2} \cdot C_{mX}^{-1}$	$mol \cdot s^{-1} \cdot kg^{-1}$	
Mitochondria-specific flux	$J_{mte,O2}$	$J_{mte,O2} = J_{V,O2} \cdot C_{mte}^{-1}$	$mol \cdot s^{-1} \cdot x_{mte}^{-1}$	10

1 The *SI* prefix k is used for the SI base unit of mass (kg = 1,000 g). In praxis, various *SI* prefixes are used for convenience, to make numbers easily readable, *e.g.* 1 mg tissue, cell or mitochondrial mass instead of 0.000001 kg.

2 In case X = cells, the sample number concentration is $C_{Ncell} = N_{cell} \cdot V^{-1}$, and volume may be expressed in [dm^3 = L] or [cm^3 = mL]. See **Table 7** for different sample types.

3 mt-concentration is an experimental variable, dependent on sample concentration: (*1*) $C_{mte} = mte \cdot V^{-1}$; (*2*) $C_{mte} = mte_X \cdot C_{NX}$; (*3*) $C_{mte} = C_{mX} \cdot D_{mte}$.

4 If the amount of mitochondria, mte, is expressed as mitochondrial mass, then D_{mte} is the mass fraction of mitochondria in the sample. If mte is expressed as mitochondrial volume, V_{mt}, and the

mass of sample, m_X, is replaced by volume of sample, V_X, then D_{mte} is the volume fraction of mitochondria in the sample.

5 $mte_X = mte \cdot N_X^{-1} = C_{mte} \cdot C_{NX}^{-1}$.

6 Entity O_2 can be replaced by other chemical entities B to study different reactions.

7 I_{O2} and V are defined per instrument chamber as a system of constant volume (and constant temperature), which may be closed or open. I_{O2} is abbreviated for $I_{O2,r}$, *i.e.* the metabolic or internal O_2 flow of the chemical reaction r in which O_2 is consumed, hence the negative stoichiometric number, $\nu_{O2} = -1$. $I_{O2,r} = d_r n_{O2}/dt \cdot \nu_{O2}^{-1}$. If r includes all chemical reactions in which O_2 participates, then $d_r n_{O2} = dn_{O2} - d_e n_{O2}$, where dn_{O2} is the change in the amount of O_2 in the instrument chamber and $d_e n_{O2}$ is the amount of O_2 added externally to the system. At steady state, by definition $dn_{O2} = 0$, hence $d_r n_{O2} = -d_e n_{O2}$.

8 $J_{V,O2}$ is an experimental variable, expressed per volume of the instrument chamber.

9 $I_{X,O2}$ is a physiological variable, depending on the size of entity X.

10 There are many ways to normalize for a mitochondrial marker, that are used in different experimental approaches: (*1*) $J_{mte,O2} = J_{V,O2} \cdot C_{mte}^{-1}$; (*2*) $J_{mte,O2} = J_{V,O2} \cdot C_{mX}^{-1} \cdot D_{mte}^{-1} = J_{mX,O2} \cdot D_{mte}^{-1}$; (*3*) $J_{mte,O2} = J_{V,O2} \cdot C_{NX}^{-1} \cdot mte_X^{-1} = I_{X,O2} \cdot mte_X^{-1}$; (*4*) $J_{mte,O2} = I_{O2} \cdot mte^{-1}$.

Mass-specific flux, $J_{mX,O2}$: Mass-specific flux is obtained by expressing respiration per mass of sample, m_X [mg]. X is the type of sample, *e.g.*, tissue homogenate, permeabilized fibres or cells. Volume-specific flux is divided by mass concentration of X, $J_{mX,O2} = J_{V,O2}/C_{mX}$; or flow per cell is divided by mass per cell, $J_{mcell,O2} = I_{cell,O2}/M_{cell}$. If mass-specific O_2 flux is constant and independent of sample size (expressed as mass), then there is no interaction between the subsystems. A 1.5 mg and a 3.0 mg muscle sample respires at identical mass-specific flux. Mass-specific O_2 flux, however, may change with the mass of a tissue sample, cells or isolated mitochondria in the measuring chamber, in which case the nature of the interaction becomes an issue. Optimization of cell density and arrangement is generally important and particularly in experiments carried out in wells, considering the confluency of the cell monolayer or clumps of cells (Salabei *et al.* 2014).

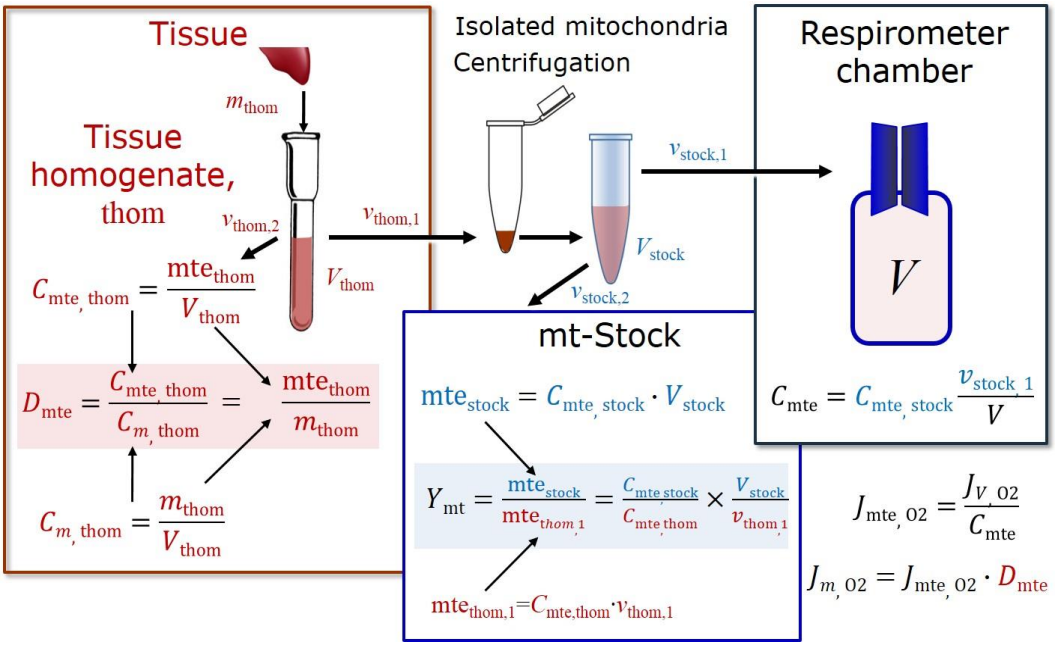

1072

Symbol	Definition [Units]
C_{mte}	Mitochondrial concentration in chamber [$x_{mte} \cdot L^{-1}$]
C_m	Sample mass concentration in chamber [$g \cdot L^{-1}$]
D_{mte}	Specific mte-density per tissue mass [$x_{mte} \cdot g^{-1}$]
$J_{m,O2}$	Mass-specific O_2 flux [$nmol \cdot s^{-1} \cdot g^{-1}$]
$J_{mte,O2}$	Mitochondria-specific O_2 flux [$nmol \cdot s^{-1} \cdot x_{mte}^{-1}$]
mte	Amount of mitochondrial elements [x_{mte}]
m_{thom}	Mass of tissue in the homogenate [g]
Y_{mt}	Yield of isolated mitochondria

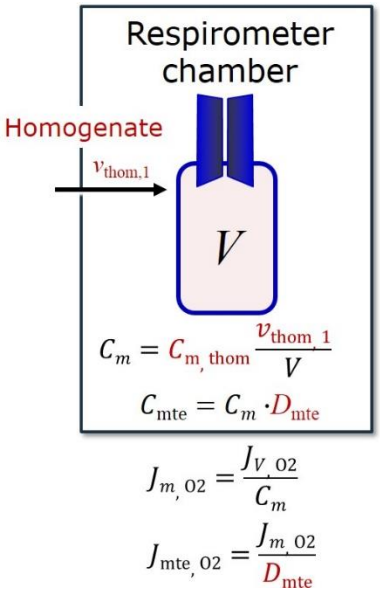

1073

1074 **Fig. 8. Normalization of volume-specific flux of isolated mitochondria and tissue**
1075 **homogenate. A:** Mitochondrial yield, Y_{mt}, in preparation of isolated mitochondria. $v_{thom,1}$
1076 and $v_{stock,1}$ are the volumes transferred from the total volume, V_{thom} and V_{stock}, respectively.
1077 $mte_{thom,1}$ is the amount of mitochondrial elements in volume $v_{thom,1}$ used for isolation. **B:**
1078 In respirometry with homogenate, $v_{thom,1}$ is transferred directly into the respirometer
1079 chamber. See **Table 6** for further explanation of symbols.

1080

1081

1082

Table 7. Some useful abbreviations of various sample types, *X*.

Identity of sample	*X*
Mitochondrial preparation	mtprep
Isolated mitochondria	imt
Tissue homogenate	thom
Permeabilized tissue	pti
Permeabilized fibre	pfi
Permeabilized cell	pce
Cell	ce
Organism	org

Number concentration, C_{NX}: The experimental *number concentration* of sample in the case of cells or animals, *e.g.*, nematodes is $C_{NX} = N_X/V$ [x·mL^{-1}], where N_X is the number of cells or organisms in the chamber (**Table 6**).

Flow per sample entity, $I_{X,O2}$: A special case of normalization is encountered in respiratory studies with permeabilized (or intact) cells. If respiration is expressed per cell, the O_2 flow per measurement system is replaced by the O_2 flow per cell, $I_{cell,O2}$ (**Table 6**). O_2 flow can be calculated from volume-specific O_2 flux, $J_{V,O2}$ [nmol·s^{-1}·L^{-1}] (per V of the measurement chamber [L]), divided by the number concentration of cells, $C_{Nce} = N_{ce}/V$ [cell·L^{-1}], where N_{ce} is the number of cells in the chamber. Cellular O_2 flow can be compared between cells of identical size. To take into account changes and differences in cell size, further normalization is required to obtain cell size-specific or mitochondrial marker-specific O_2 flux (Renner *et al.* 2003).

The complexity changes when the sample is a whole organism studied as an experimental model. The well-established scaling law in respiratory physiology reveals a strong interaction of O_2 consumption and individual body mass of an organism, since *basal* metabolic rate (flow) does not increase linearly with body mass, whereas *maximum* mass-specific O_2 flux, $\dot{V}_{O2max}$ or

$\dot{V}_{O2peak}$, is approximately constant across a large range of individual body mass (Weibel and Hoppeler 2005), with individuals, breeds, and certain species deviating substantially from this general relationship. $\dot{V}_{O2peak}$ of human endurance athletes is 60 to 80 mL $O_2 \cdot min^{-1} \cdot kg^{-1}$ body mass, converted to $J_{m,O2peak}$ of 45 to 60 $nmol \cdot s^{-1} \cdot g^{-1}$ (Gnaiger 2014; **Table 8**).

4.3. Normalization for mitochondrial content

Normalization is a problematic subject and it is essential to consider the question of the study. If the study aims to compare tissue performance, such as the effects of a certain treatment on a specific tissue, then normalization can be successful, using tissue mass or protein content, for example. If the aim, however, is to find differences of mitochondrial function independent of mitochondrial density (**Table 6**), then normalization to a mitochondrial marker is imperative (**Fig. 9**). However, one cannot assume that quantitative changes in various markers such as mitochondrial proteins necessarily occur in parallel with one another. It is important to first establish that the marker chosen is not selectively altered by the performed treatment. In conclusion, the normalization must reflect the question under investigation to reach a satisfying answer. On the other hand, the goal of comparing results across projects and institutions requires some standardization on normalization for entry into a databank.

Mitochondrial concentration, C_{mte}, and mitochondrial markers: It is important that mitochondrial concentration in the tissue and the measurement chamber be quantified, as a physiological output and result of mitochondrial biogenesis and degradation, and as a quantity for normalization in functional analyses. Mitochondrial organelles comprise a cellular reticulum that is in a continual flux of fusion and fission. Hence the definition of an "amount" of mitochondria is often misconceived: mitochondria cannot be counted as a number of occurring elements. Therefore, quantification of the "amount" of mitochondria depends on measurement of chosen mitochondrial markers. ‘Mitochondria are the structural and functional elemental units of cell respiration’ (Gnaiger 2014). The quantity of a mitochondrial marker can

be considered as the measurement of the amount of *elemental mitochondrial units* or *mitochondrial elements*, mte. However, since mitochondrial quality changes under certain stimuli, particularly in mitochondrial dysfunction and after exercise training (Pesta *et al.* 2011; Campos *et al.* 2017), some markers can vary while other markers are unchanged. (*1*) Mitochondrial volume and membrane area are structural markers, whereas mitochondrial protein mass is frequently used as a marker for isolated mitochondria. (*2*) Molecular and enzymatic mitochondrial markers (amounts or activities) can be selected as matrix markers, *e.g.*, citrate synthase activity, mtDNA; mtIM-markers, *e.g.*, cytochrome *c* oxidase activity, aa_3 content, cardiolipin, or mtOM-markers, *e.g.*, TOM20. (*3*) Extending the measurement of mitochondrial marker enzyme activity to mitochondrial pathway capacity, measured as ET- or OXPHOS-capacity, can be considered as an integrative functional mitochondrial marker.

Depending on the type of mitochondrial marker, the mitochondrial elements, mte, are expressed in marker-specific units. Although concentration and density are used synonymously in physical chemistry, it is recommended to distinguish *experimental mitochondrial concentration*, C_{mte} = mte/V and *physiological mitochondrial density*, D_{mte} = mte/m_X. Then mitochondrial density is the amount of mitochondrial elements per mass of tissue (**Fig. 9**). The former is mitochondrial density multiplied by sample mass concentration, $C_{\mathrm{mte}} = D_{\mathrm{mte}} \cdot C_{mX}$, or mitochondrial content multiplied by sample number concentration, $C_{\mathrm{mte}} = \mathrm{mte}_X \cdot C_{NX}$ (**Table 6**).

Mitochondria-specific flux, $J_{\mathrm{mte,O2}}$: Volume-specific metabolic O_2 flux depends on: (*1*) the sample concentration in the volume of the instrument chamber, C_{mX}, or C_{NX}; (*2*) the mitochondrial density in the sample, D_{mte} = mte/m_X or mte_X = mte/N_X; and (*3*) the specific mitochondrial activity or performance per elemental mitochondrial unit, $J_{\mathrm{mte,O2}} = J_{V,\mathrm{O2}}/C_{\mathrm{mte}}$ (**Table 6**). Obviously, the numerical results for $J_{\mathrm{mte,O2}}$ vary according to the type of mitochondrial marker chosen for measurement of mte and C_{mte} = mte/V.

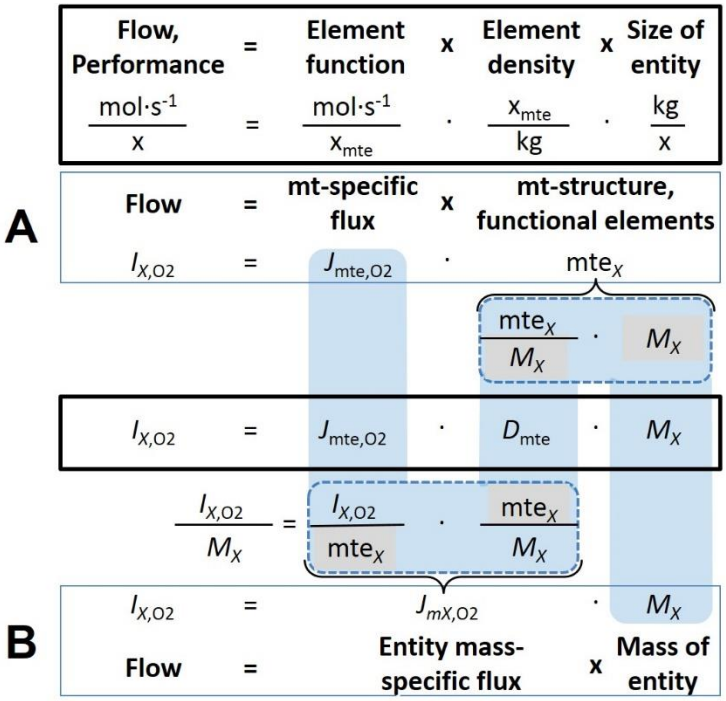

Fig. 9. Structure-function analysis of performance of an organism, organ or tissue, or a cell (sample entity *X*). O_2 flow, $I_{X,O2}$, is the product of performance per functional element (element function, mitochondria-specific flux), element density (mitochondrial density, D_{mte}), and size of entity *X* (mass M_X). (**A**) Structured analysis: performance is the product of mitochondrial *function* (mt-specific flux) and *structure* (functional elements; D_{mte} times mass of *X*). (**B**) Unstructured analysis: performance is the product of *entity mass-specific flux*, $J_{mX,O2} = I_{X,O2}/M_X = I_{O2}/m_X$ [$mol \cdot s^{-1} \cdot kg^{-1}$] and *size of entity*, expressed as mass of *X*; $M_X = m_X \cdot N_X^{-1}$ [$kg \cdot x^{-1}$]. See **Table 6** for further explanation of quantities and units. Modified from Gnaiger (2014).

4.4. Evaluation of mitochondrial markers

Different methods are implicated in quantification of mitochondrial markers and have different strengths. Some problems are common for all mitochondrial markers, mte: (*1*) Accuracy of measurement is crucial, since even a highly accurate and reproducible

measurement of O_2 flux results in an inaccurate and noisy expression normalized for a biased and noisy measurement of a mitochondrial marker. This problem is acute in mitochondrial respiration because the denominators used (the mitochondrial markers) are often very small moieties whose accurate and precise determination is difficult. This problem can be avoided when O_2 fluxes measured in substrate-uncoupler-inhibitor titration protocols are normalized for flux in a defined respiratory reference state, which is used as an *internal* marker and yields flux control ratios, *FCR*s (**Fig. 7**). *FCR*s are independent of any *externally* measured markers and, therefore, are statistically very robust, considering the limitations of ratios in general (Jasienski and Bazzaz 1999). *FCR*s indicate qualitative changes of mitochondrial respiratory control, with highest quantitative resolution, separating the effect of mitochondrial density or concentration on $J_{mX,O2}$ and $I_{X,O2}$ from that of function per elemental mitochondrial marker, $J_{mte,O2}$ (Pesta *et al.* 2011; Gnaiger 2014). (*2*) If mitochondrial quality does not change and only the amount of mitochondria, defined by the chosen mitochondrial marker, varies as a determinant of mass-specific flux, any marker is equally qualified in principle; then in practice selection of the optimum marker depends only on the accuracy and precision of measurement of the mitochondrial marker. (*3*) If mitochondrial flux control ratios change, then there may not be any best mitochondrial marker. In general, measurement of multiple mitochondrial markers enables a comparison and evaluation of normalization for a variety of mitochondrial markers. Evaluation of mitochondrial markers in healthy controls is insufficient for providing guidelines for application in the diagnosis of pathological states and specific treatments.

In line with the concept of the respiratory control ratio (Chance and Williams 1955a), the most readily used normalization is that of flux control ratios and flux control factors (Gnaiger 2014). Selection of the state of maximum flux in a protocol as the reference state has the advantages of (*1*) internal normalization, (*2*) statistical linearization of the response in the range of 0 to 1, and (*3*) consideration of maximum flux for integrating a very large number of elemental steps in the OXPHOS- or ET-pathways. This reduces the risk of selecting a functional

marker that is specifically altered by the treatment or pathodology, yet increases the chance that the highly integrative pathway is disproportionately affected, *e.g.* the OXPHOS- rather than ET-pathway in case of an enzymatic defect in the phosphorylation-pathway. In this case, additional information can be obtained by reporting flux control ratios based on a reference state which indicates stable tissue-mass specific flux. Stereological determination of mitochondrial content via two-dimensional transmission electron microscopy can have limitations due to the dynamics of mitochondrial size (Meinild Lundby *et al.* 2017). Accurate determination of three-dimensional volume by two-dimensional microscopy can be both time consuming and statistically challenging (Larsen *et al.* 2012). Using mitochondrial marker enzymes (citrate synthase activity, Complex I–IV amount or activity) for normalization of flux is limited in part by the same factors that apply to the use of flux control ratios. Strong correlations between various mitochondrial markers and citrate synthase activity (Reichmann et al. 1985; Boushel *et al.* 2007; Mogensen *et al.* 2007) are expected in a specific tissue of healthy subjects and in disease states not specifically targeting citrate synthase. Citrate synthase activity is acutely modifiable by exercise (Tonkonogi *et al.* 1997; Leek *et al.* 2001). Evaluation of mitochondrial markers related to a selected age and sex cohort cannot be extrapolated to provide recommendations for normalization in respirometric diagnosis of disease, in different states of development and ageing, different cell types, tissues, and species. mtDNA normalised to nDNA via qPCR is correlated to functional mitochondrial markers including OXPHOS- and ET-capacity in some cases (Puntschart *et al.* 1995; Wang *et al.* 1999; Menshikova *et al.* 2006; Boushel *et al.* 2007), but lack of such correlations have been reported (Menshikova *et al.* 2005; Schultz and Wiesner 2000; Pesta *et al.* 2011). Several studies indicate a strong correlation between cardiolipin content and increase in mitochondrial functionality with exercise (Menshikova *et al.* 2005; Menshikova *et al.* 2007; Larsen *et al.* 2012; Faber *et al.* 2014), but its use as a general mitochondrial biomarker in disease remains questionable.

4.5. Conversion: units and normalization

Many different units have been used to report the rate of oxygen consumption, OCR (**Table 8**). *SI* base units provide the common reference for introducing the theoretical principles (**Fig. 7**), and are used with appropriately chosen *SI* prefixes to express numerical data in the most practical format, with an effort towards unification within specific areas of application (**Table 9**). For studies of cells, we recommend that respiration be expressed, as far as possible, as (*1*) O_2 flux normalized for a mitochondrial marker, for separation of the effects of mitochondrial quality and content on cell respiration (this includes *FCR*s as a normalization for a functional mitochondrial marker); (*2*) O_2 flux in units of cell volume or mass, for comparison of respiration of cells with different cell size (Renner *et al.* 2003) and with studies on tissue preparations, and (*3*) O_2 flow in units of attomole (10^{-18} mol) of O_2 consumed by each cell in a second [amol·s^{-1}·$cell^{-1}$], numerically equivalent to [pmol·s^{-1}·10^{-6} cells]. This convention allows information to be easily used when designing experiments in which oxygen consumption must be considered. For example, to estimate the volume-specific O_2 flux in an instrument chamber that would be expected at a particular cell number concentration, one simply needs to multiply the flow per cell by the number of cells per volume of interest. This provides the amount of O_2 [mol] consumed per time [s^{-1}] per unit volume [L^{-1}]. At an O_2 flow of 100 amol·s^{-1}·$cell^{-1}$ and a cell density of 10^9 cells·L^{-1} (10^6 cells·mL^{-1}), the volume-specific O_2 flux is 100 nmol·s^{-1}·L^{-1} (100 pmol·s^{-1}·mL^{-1}).

Although volume is expressed as m^3 using the *SI* base unit, the litre [dm^3] is the basic unit of volume for concentration and is used for most solution chemical kinetics. If one multiplies $I_{cell,O2}$ by C_{Ncell}, then the result will not only be the amount of O_2 [mol] consumed per time [s^{-1}] in one litre [L^{-1}], but also the change in the concentration of oxygen per second (for any volume of an ideally closed system). This is ideal for kinetic modeling as it blends with chemical rate equations where concentrations are typically expressed in mol·L^{-1} (Wagner *et al.* 2011). In studies of multinuclear cells, such as differentiated skeletal muscle cells, it is easy to determine

the number of nuclei but not the total number of cells. A generalized concept, therefore, is obtained by substituting cells by nuclei as the sample entity. This does not hold, however, for enucleated platelets.

Table 8. Conversion of various units used in respirometry and ergometry. e is the number of electrons or reducing equivalents. z_B is the charge number of entity B.

1 Unit	x	Multiplication factor	*SI*-Unit	Note
ng.atom O·s^{-1}	(2 e)	0.5	nmol O_2·s^{-1}	
ng.atom O·min^{-1}	(2 e)	8.33	pmol O_2·s^{-1}	
natom O·min^{-1}	(2 e)	8.33	pmol O_2·s^{-1}	
nmol O_2·min^{-1}	(4 e)	16.67	pmol O_2·s^{-1}	
nmol O_2·h^{-1}	(4 e)	0.2778	pmol O_2·s^{-1}	
mL O_2·min^{-1} at STPD[a]		0.744	µmol O_2·s^{-1}	1
W = J/s at -470 kJ/mol O_2		-2.128	µmol O_2·s^{-1}	
mA = mC·s^{-1}	(z_{H+} = 1)	10.36	nmol H^+·s^{-1}	2
mA = mC·s^{-1}	(z_{O2} = 4)	2.59	nmol O_2·s^{-1}	2
nmol H^+·s^{-1}	(z_{H+} = 1)	0.09649	mA	3
nmol O_2·s^{-1}	(z_{O2} = 4)	0.38594	mA	3

1 At standard temperature and pressure dry (STPD: 0 °C = 273.15 K and 1 atm = 101.325 kPa = 760 mmHg), the molar volume of an ideal gas, V_m, and $V_{m,O2}$ is 22.414 and 22.392 L.mol^{-1} respectively. Rounded to three decimal places, both values yield the conversion factor of 0.744. For comparison at NTPD (20 °C), $V_{m,O2}$ is 24.038 L.mol^{-1}. Note that the *SI* standard pressure is 100 kPa.

2 The multiplication factor is $10^6/(z_B \cdot F)$.

3 The multiplication factor is $z_B \cdot F/10^6$.

4.5. Conversion: oxygen, proton and ATP flux

$J_{O2,k}$ is coupled in mitochondrial steady states to proton cycling, $J_{\infty H+} = J_{H+,out} = J_{H+,in}$ (**Fig. 2**). $J_{H+,out/n}$ and $J_{H+,in/n}$ [nmol·s^{-1}·L^{-1}] are converted into electrical units, $J_{H+,out/e}$ [mC·s^{-1}·L^{-1} = mA·L^{-1}] = $J_{H+,out/n}$ [nmol·s^{-1}·L^{-1}]·F [C·mol^{-1}]·10^{-6} (**Table 4**). At a $J_{H+,out}/J_{O2,k}$ ratio or H^+_{out}/O_2 of 20 (H^+_{out}/O = 10), a volume-specific O_2 flux of 100 nmol·s^{-1}·L^{-1} would correspond to a proton flux of 2,000 nmol H^+_{out}·s^{-1}·L^{-1} or volume-specific current of 193 mA·L^{-1}.

$$J_{V,H+out/e}\ [mA·L^{-1}] = J_{V,H+out/n}·F·10^{-6}\ [nmol·s^{-1}·L^{-1}·mC·nmol^{-1}] \quad \text{(Eq. 3.1)}$$

$$J_{V,H+out/e}\ [mA·L^{-1}] = J_{V,O2}·(H^+_{out}/O_2)·F·10^{-6}\ [mC·s^{-1}·L^{-1} = mA·L^{-1}] \quad \text{(Eq. 3.2)}$$

Table 9. Conversion of units with preservation of numerical values.

Name	Frequently used unit	Equivalent unit	Note
Volume-specific flux, $J_{V,O2}$	pmol·s^{-1}·mL^{-1}	nmol·s^{-1}·L^{-1}	1
	mmol·s^{-1}·L^{-1}	mol·s^{-1}·m^{-3}	
Cell-specific flow, I_{O2}	pmol·s^{-1}·10^{-6} cells	amol·s^{-1}·cell^{-1}	2
	pmol·s^{-1}·10^{-9} cells	zmol·s^{-1}·cell^{-1}	3
Cell number concentration, C_{Nce}	10^6 cells·mL^{-1}	10^9 cells·L^{-1}	
Mitochondrial protein concentration, C_{mte}	0.1 mg·mL^{-1}	0.1 g·L^{-1}	
Mass-specific flux, $J_{m,O2}$	pmol·s^{-1}·mg^{-1}	nmol·s^{-1}·g^{-1}	4
Catabolic power, $P_{O2,k}$	µW·10^{-6} cells	pW·cell^{-1}	1
Volume	1,000 L	m^3 (1,000 kg)	
	L	dm^3 (kg)	
	mL	cm^3 (g)	
	µL	mm^3 (mg)	
	fL	µm^3 (pg)	
Amount of substance concentration	M = mol·L^{-1}	mol·dm^{-3}	

1 pmol: picomole = 10^{-12} mol
2 amol: attomole = 10^{-18} mol
3 zmol: zeptomole = 10^{-21} mol
4 nmol: nanomole = 10^{-9} mol

ET-capacity in various human cell types including HEK 293, primary HUVEC and fibroblasts ranges from 50 to 180 amol·s^{-1}·cell^{-1}, measured in intact cells in the noncoupled state (see Gnaiger 2014). At 100 amol·s^{-1}·cell^{-1} corrected for ROX (corresponding to a catabolic power of -48 pW·cell^{-1}), the current across the mt-membranes, I_e, approximates 193 pA·cell^{-1} or 0.2

nA per cell. See Rich (2003) for an extension of quantitative bioenergetics from the molecular to the human scale, with a transmembrane proton flux equivalent to 520 A in an adult at a catabolic power of -110 W. Modelling approaches illustrate the link between proton motive force and currents (Willis *et al.* 2016).For NADH- and succinate-linked respiration, the mechanistic P»/O_2 ratio (referring to the full 4 electron reduction of O_2) is calculated at 20/3.7 and 12/3.7, respectively (Eq. 4) equal to 5.4 and 3.3. The classical P»/O ratios (referring to the 2 electron reduction of 0.5 O_2) are 2.7 and 1.6 (Watt *et al.* 2010), in direct agreement with the measured P»/O ratio for succinate of 1.58 ± 0.02 (Gnaiger *et al.* 2000; for detailed reviews see Wikström and Hummer 2012; Sazanov 2015),

$$P\text{»}/O_2 = (H^+_{out}/O_2)/(H^+_{in}/P\text{»}) \quad \text{(Eq. 4)}$$

In summary (**Fig. 1**),

$$J_{V,P\text{»}}\ [\text{nmol}\cdot\text{s}^{-1}\cdot\text{L}^{-1}] = J_{V,O2}\cdot(H^+_{out}/O_2)/(\ H^+_{in}/P\text{»}) \quad \text{(Eq. 5.1)}$$

$$J_{V,P\text{»}}\ [\text{nmol}\cdot\text{s}^{-1}\cdot\text{L}^{-1}] = J_{V,O2}\cdot(P\text{»}/O_2) \quad \text{(Eq. 5.2)}$$

We consider isolated mitochondria as powerhouses and proton pumps as molecular machines to relate experimental results to energy metabolism of the intact cell. The cellular P»/O_2 based on oxidation of glycogen is increased by the glycolytic (fermentative) substrate-level phosphorylation of 3 P»/Glyc, *i.e.*, 0.5 mol P» for each mol O_2 consumed in the complete oxidation of a mol glycosyl unit (Glyc). Adding 0.5 to the mitochondrial P»/O_2 ratio of 5.4 yields a bioenergetic cell physiological P»/O_2 ratio close to 6. Two NADH equivalents are formed during glycolysis and transported from the cytosol into the mitochondrial matrix, either by the malate-aspartate shuttle or by the glycerophosphate shuttle resulting in different theoretical yield of ATP generated by mitochondria, the energetic cost of which potentially must be taken into account. Considering also substrate-level phosphorylation in the TCA cycle, this high P»/O_2 ratio not only reflects proton translocation and OXPHOS studied in isolation, but integrates mitochondrial physiology with energy transformation in the living cell (Gnaiger 1993a).

5. Conclusions

MitoEAGLE can serve as a gateway to better diagnose mitochondrial respiratory defects linked to genetic variation, age-related health risks, sex-specific mitochondrial performance, lifestyle with its effects on degenerative diseases, and thermal and chemical environment. The present recommendations on coupling control states and rates, linked to the concept of the protonmotive force (Part 1) will be extended in a series of reports on pathway control of mitochondrial respiration, respiratory states in intact cells, and harmonization of experimental procedures.

Box 5: Mitochondrial and cell respiration

Mitochondrial and cell respiration is the process of highly exergonic and exothermic energy transformation in which scalar redox reactions are coupled to vectorial ion translocation across a semipermeable membrane, which separates the small volume of a bacterial cell or mitochondrion from the larger volume of its surroundings. The electrochemical exergy can be partially conserved in the phosphorylation of ADP to ATP or in ion pumping, or dissipated in an electrochemical short-circuit. Respiration is thus clearly distinguished from fermentation as the counterpart of cellular core energy metabolism. Respiration is separated in mitochondrial preparations from the partial contribution of fermentative pathways of the intact cell. According to this definition, residual oxygen consumption, as measured after inhibition of mitochondrial electron transfer, does not belong to the class of catabolic reactions and is, therefore, subtracted from total oxygen consumption to obtain baseline-corrected respiration.

The optimal choice for expressing mitochondrial and cell respiration (**Box 5**) as O_2 flow per biological system, and normalization for specific tissue-markers (volume, mass, protein) and mitochondrial markers (volume, protein, content, mtDNA, activity of marker enzymes,

respiratory reference state) is guided by the scientific question under study. Interpretation of the obtained data depends critically on appropriate normalization, and therefore reporting rates merely as $nmol \cdot s^{-1}$ is discouraged, since it restricts the analysis to intra-experimental comparison of relative (qualitative) differences. Expressing O_2 consumption per cell may not be possible when dealing with tissues. For studies with mitochondrial preparations, we recommend that normalizations be provided as far as possible: (*1*) on a per cell basis as O_2 flow (a biophysical normalization); (*2*) per g cell or tissue protein, or per cell or tissue mass as mass-specific O_2 flux (a cellular normalization); and (*3*) per mitochondrial marker as mt-specific flux (a mitochondrial normalization). With information on cell size and the use of multiple normalizations, maximum potential information is available (Renner *et al.* 2003; Wagner *et al.* 2011; Gnaiger 2014). When using isolated mitochondria, mitochondrial protein is a frequently applied mitochondrial marker, the use of which is basically restricted to isolated mitochondria. Mitochondrial markers, such as citrate synthase activity as an enzymatic matrix marker, provide a link to the tissue of origin on the basis of calculating the mitochondrial yield, *i.e.*, the fraction of mitochondrial marker obtained from a unit mass of tissue.

Acknowledgements

We thank M. Beno for management assistance. Supported by COST Action CA15203 MitoEAGLE and K-Regio project MitoFit (EG).

Competing financial interests: E.G. is founder and CEO of Oroboros Instruments, Innsbruck, Austria.

6. References (*incomplete; www links will be deleted in the final version*)

Altmann R. Die Elementarorganismen und ihre Beziehungen zu den Zellen. Zweite vermehrte Auflage. Verlag Von Veit & Comp, Leipzig 1894;160 pp. - www.mitoeagle.org/index.php/Altmann_1894_Verlag_Von_Veit_%26_Comp

1364 Birkedal R, Laasmaa M, Vendelin M. The location of energetic compartments affects
1365 energetic communication in cardiomyocytes. Front Physiol 2014;5:376. doi:
1366 10.3389/fphys.2014.00376. eCollection 2014. PMID: 25324784
1367 Breton S, Beaupré HD, Stewart DT, Hoeh WR, Blier PU. The unusual system of doubly
1368 uniparental inheritance of mtDNA: isn't one enough? Trends Genet 2007;23:465-74.
1369 Brown GC. Control of respiration and ATP synthesis in mammalian mitochondria and cells.
1370 Biochem J 1992;284:1-13. - www.mitoeagle.org/index.php/Brown_1992_Biochem_J
1371 Campos JC, Queliconi BB, Bozi LHM, Bechara LRG, Dourado PMM, Andres AM, Jannig
1372 PR, Gomes KMS, Zambelli VO, Rocha-Resende C, Guatimosim S, Brum PC, Mochly-
1373 Rosen D, Gottlieb RA, Kowaltowski AJ, Ferreira JCB. Exercise reestablishes
1374 autophagic flux and mitochondrial quality control in heart failure. Autophagy
1375 2017;13:1304-317.
1376 Chance B, Williams GR. Respiratory enzymes in oxidative phosphorylation. I. Kinetics of
1377 oxygen utilization. J Biol Chem 1955a;217:383-93. -
1378 http://www.mitoeagle.org/index.php/Chance_1955_J_Biol_Chem-I
1379 Chance B, Williams GR. Respiratory enzymes in oxidative phosphorylation: III. The steady
1380 state. J Biol Chem 1955b;217:409-27. -
1381 www.mitoeagle.org/index.php/Chance_1955_J_Biol_Chem-III
1382 Chance B, Williams GR. Respiratory enzymes in oxidative phosphorylation. IV. The
1383 respiratory chain. J Biol Chem 1955c;217:429-38. -
1384 www.mitoeagle.org/index.php/Chance_1955_J_Biol_Chem-IV
1385 Chance B, Williams GR. The respiratory chain and oxidative phosphorylation. Adv Enzymol
1386 Relat Subj Biochem 1956;17:65-134. -
1387 www.mitoeagle.org/index.php/Chance_1956_Adv_Enzymol_Relat_Subj_Biochem
1388 Cobb LJ, Lee C, Xiao J, Yen K, Wong RG, Nakamura HK, Mehta HH, Gao Q, Ashur C,
1389 Huffman DM, Wan J, Muzumdar R, Barzilai N, Cohen P. Naturally occurring

mitochondrial-derived peptides are age-dependent regulators of apoptosis, insulin sensitivity, and inflammatory markers. Aging (Albany NY) 2016;8:796-809.

Cohen ER, Cvitas T, Frey JG, Holmström B, Kuchitsu K, Marquardt R, Mills I, Pavese F, Quack M, Stohner J, Strauss HL, Takami M, Thor HL. Quantities, units and smbols in physical chemistry, IUPAC Green Book 2008;3rd Edition, 2nd Printing, IUPAC & RSC Publishing, Cambridge. - www.mitoeagle.org/index.php/Cohen_2008_IUPAC_Green_Book

Cooper H, Hedges LV, Valentine JC (eds). The handbook of research synthesis and meta-analysis. Russell Sage Foundation 2009.

Coopersmith J. Energy, the subtle concept. The discovery of Feynman's blocks from Leibnitz to Einstein. Oxford University Press 2010;400 pp.

Cummins J. Mitochondrial DNA in mammalian reproduction. Rev Reprod 1998;3:172–82.

Dai Q, Shah AA, Garde RV, Yonish BA, Zhang L, Medvitz NA, Miller SE, Hansen EL, Dunn CN, Price TM. A truncated progesterone receptor (PR-M) localizes to the mitochondrion and controls cellular respiration. Mol Endocrinol 2013;27:741-53.

Duarte FV, Palmeira CM, Rolo AP. The role of microRNAs in mitochondria: small players acting wide. Genes (Basel) 2014;5:865-86.

Dufour S, Rousse N, Canioni P, Diolez P. Top-down control analysis of temperature effect on oxidative phosphorylation. Biochem J 1996;314:743-51.

Ernster L, Schatz G Mitochondria: a historical review. J Cell Biol 1981;91:227s-55s. - www.mitoeagle.org/index.php/Ernster_1981_J_Cell_Biol

Estabrook RW. Mitochondrial respiratory control and the polarographic measurement of ADP:O ratios. Methods Enzymol 1967;10:41-7. - www.mitoeagle.org/index.php/Estabrook_1967_Methods_Enzymol

Faber C, Zhu ZJ, Castellino S, Wagner DS, Brown RH, Peterson RA, Gates L, Barton J, Bickett M, Hagerty L, Kimbrough C, Sola M, Bailey D, Jordan H, Elangbam CS.

Cardiolipin profiles as a potential biomarker of mitochondrial health in diet-induced obese mice subjected to exercise, diet-restriction and ephedrine treatment. J Appl Toxicol 2014;34:1122-9.

Fell D. Understanding the control of metabolism. Portland Press 1997.

Garlid KD, Semrad C, Zinchenko V. Does redox slip contribute significantly to mitochondrial respiration? In: Schuster S, Rigoulet M, Ouhabi R, Mazat J-P (eds) Modern trends in biothermokinetics. Plenum Press, New York, London 1993;287-93.

Gerö D, Szabo C. Glucocorticoids suppress mitochondrial oxidant production via upregulation of uncoupling protein 2 in hyperglycemic endothelial cells. PLoS One 2016;11:e0154813.

Gnaiger E. Efficiency and power strategies under hypoxia. Is low efficiency at high glycolytic ATP production a paradox? In: Surviving Hypoxia: Mechanisms of Control and Adaptation. Hochachka PW, Lutz PL, Sick T, Rosenthal M, Van den Thillart G (eds.) CRC Press, Boca Raton, Ann Arbor, London, Tokyo 1993a:77-109. - www.mitoeagle.org/index.php/Gnaiger_1993_Hypoxia

Gnaiger E. Nonequilibrium thermodynamics of energy transformations. Pure Appl Chem 1993b;65:1983-2002. - www.mitoeagle.org/index.php/Gnaiger_1993_Pure_Appl_Chem

Gnaiger E. Bioenergetics at low oxygen: dependence of respiration and phosphorylation on oxygen and adenosine diphosphate supply. Respir Physiol 2001;128:277-97. - www.mitoeagle.org/index.php/Gnaiger_2001_Respir_Physiol

Gnaiger E. Mitochondrial pathways and respiratory control. An introduction to OXPHOS analysis. 4th ed. Mitochondr Physiol Network 2014;19.12. Oroboros MiPNet Publications, Innsbruck:80 pp. - www.mitoeagle.org/index.php/Gnaiger_2014_MitoPathways

Gnaiger E. Capacity of oxidative phosphorylation in human skeletal muscle. New perspectives of mitochondrial physiology. Int J Biochem Cell Biol 2009;41:1837-45. - www.mitoeagle.org/index.php/Gnaiger_2009_Int_J_Biochem_Cell_Biol

Gnaiger E, Méndez G, Hand SC. High phosphorylation efficiency and depression of uncoupled respiration in mitochondria under hypoxia. Proc Natl Acad Sci USA 2000;97:11080-5. - www.mitoeagle.org/index.php/Gnaiger_2000_Proc_Natl_Acad_Sci_U_S_A

Greggio C, Jha P, Kulkarni SS, Lagarrigue S, Broskey NT, Boutant M, Wang X, Conde Alonso S, Ofori E, Auwerx J, Cantó C, Amati F. Enhanced respiratory chain supercomplex formation in response to exercise in human skeletal muscle. Cell Metab 2017;25:301-11. - http://www.mitoeagle.org/index.php/Greggio_2017_Cell_Metab

Hofstadter DR. Gödel, Escher, Bach: An eternal golden braid. A metaphorical fugue on minds and machines in the spirit of Lewis Carroll. Harvester Press 1979;499 pp. - www.mitoeagle.org/index.php/Hofstadter_1979_Harvester_Press

Illaste A, Laasmaa M, Peterson P, Vendelin M. Analysis of molecular movement reveals latticelike obstructions to diffusion in heart muscle cells. Biophys J 2012;102:739-48. - PMID: 22385844

Jasienski M, Bazzaz FA. The fallacy of ratios and the testability of models in biology. Oikos 1999;84:321-26.

Jepihhina N, Beraud N, Sepp M, Birkedal R, Vendelin M. Permeabilized rat cardiomyocyte response demonstrates intracellular origin of diffusion obstacles. Biophys J 2011;101:2112-21. - PMID: 22067148

Klepinin A, Ounpuu L, Guzun R, Chekulayev V, Timohhina N, Tepp K, Shevchuk I, Schlattner U, Kaambre T. Simple oxygraphic analysis for the presence of adenylate kinase 1 and 2 in normal and tumor cells. J Bioenerg Biomembr 2016;48:531-48. - http://www.mitoeagle.org/index.php/Klepinin_2016_J_Bioenerg_Biomembr

Klingenberg M. UCP1 - A sophisticated energy valve. Biochimie 2017;134:19-27

Koit A, Shevchuk I, Ounpuu L, Klepinin A, Chekulayev V, Timohhina N, Tepp K, Puurand M,Truu L, Heck K, Valvere V, Guzun R, Kaambre T. Mitochondrial respiration in human colorectal and breast cancer clinical material is regulated differently. Oxid Med Cell Longev 2017;1372640. - http://www.mitoeagle.org/index.php/Koit_2017_Oxid_Med_Cell_Longev

Komlódi T, Tretter L. Methylene blue stimulates substrate-level phosphorylation catalysed by succinyl-CoA ligase in the citric acid cycle. Neuropharmacology 2017;123:287-98. - www.mitoeagle.org/index.php/Komlodi_2017_Neuropharmacology

Lane N. Power, sex, suicide: Mitochondria and the meaning of life. Oxford University Press 2005;354 pp.

Larsen S, Nielsen J, Neigaard Nielsen C, Nielsen LB, Wibrand F, Stride N, Schroder HD, Boushel RC, Helge JW, Dela F, Hey-Mogensen M. Biomarkers of mitochondrial content in skeletal muscle of healthy young human subjects. J Physiol 590;2012:3349-60. - http://www.mitoeagle.org/index.php/Larsen_2012_J_Physiol

Lee C, Zeng J, Drew BG, Sallam T, Martin-Montalvo A, Wan J, Kim SJ, Mehta H, Hevener AL, de Cabo R, Cohen P. The mitochondrial-derived peptide MOTS-c promotes metabolic homeostasis and reduces obesity and insulin resistance. Cell Metab 2015;21:443-54.

Lee SR, Kim HK, Song IS, Youm J, Dizon LA, Jeong SH, Ko TH, Heo HJ, Ko KS, Rhee BD, Kim N, Han J. Glucocorticoids and their receptors: insights into specific roles in mitochondria. Prog Biophys Mol Biol 2013;112:44-54.

Leek BT, Mudaliar SR, Henry R, Mathieu-Costello O, Richardson RS. Effect of acute exercise on citrate synthase activity in untrained and trained human skeletal muscle. Am J Physiol Regul Integr Comp Physiol 2001;280:R441-7.

Lemieux H, Blier PU, Gnaiger E. Remodeling pathway control of mitochondrial respiratory capacity by temperature in mouse heart: electron flow through the Q-junction in permeabilized fibers. Sci Rep 2017;7:2840. - www.mitoeagle.org/index.php/Lemieux_2017_Sci_Rep

Lenaz G, Tioli G, Falasca AI, Genova ML. Respiratory supercomplexes in mitochondria. In: Mechanisms of primary energy trasduction in biology. M Wikstrom (ed) Royal Society of Chemistry Publishing, London, UK 2017:296-337 (in press)

Margulis L. Origin of eukaryotic cells. New Haven: Yale University Press 1970.

Meinild Lundby AK, Jacobs RA, Gehrig S, de Leur J, Hauser M, Bonne TC, Flück D, Dandanell S, Kirk N, Kaech A, Ziegler U, Larsen S, Lundby C. Exercise training increases skeletal muscle mitochondrial volume density by enlargement of existing mitochondria and not de novo biogenesis. Acta Physiol (Oxf) 2017;[Epub ahead of print].

Menshikova EV, Ritov VB, Fairfull L, Ferrell RE, Kelley DE, Goodpaster BH. Effects of exercise on mitochondrial content and function in aging human skeletal muscle. J Gerontol A Biol Sci Med Sci 2006;61:534-40.

Menshikova EV, Ritov VB, Ferrell RE, Azuma K, Goodpaster BH, Kelley DE. Characteristics of skeletal muscle mitochondrial biogenesis induced by moderate-intensity exercise and weight loss in obesity. J Appl Physiol (1985) 2007;103:21-7.

Menshikova EV, Ritov VB, Toledo FG, Ferrell RE, Goodpaster BH, Kelley DE. Effects of weight loss and physical activity on skeletal muscle mitochondrial function in obesity. Am J Physiol Endocrinol Metab 2005;288:E818-25.

Miller GA. The science of words. Scientific American Library New York 1991;276 pp. - www.mitoeagle.org/index.php/Miller_1991_Scientific_American_Library

Mitchell P. Chemiosmotic coupling in oxidative and photosynthetic phosphorylation Biochim Biophys Acta Bioenergetics 2011;1807:1507-38. - http://www.sciencedirect.com/science/article/pii/S0005272811002283

Mitchell P, Moyle J. Respiration-driven proton translocation in rat liver mitochondria. Biochem J 1967;105:1147-62. - www.mitoeagle.org/index.php/Mitchell_1967_Biochem_J

Mogensen M, Sahlin K, Fernström M, Glintborg D, Vind BF, Beck-Nielsen H, Højlund K. Mitochondrial respiration is decreased in skeletal muscle of patients with type 2 diabetes. Diabetes 2007;56:1592-9.

Moreno M, Giacco A, Di Munno C, Goglia F. Direct and rapid effects of 3,5-diiodo-L-thyronine (T2). Mol Cell Endocrinol 2017;7207:30092-8.

Morrow RM, Picard M, Derbeneva O, Leipzig J, McManus MJ, Gouspillou G, Barbat-Artigas S, Dos Santos C, Hepple RT, Murdock DG, Wallace DC. Mitochondrial energy deficiency leads to hyperproliferation of skeletal muscle mitochondria and enhanced insulin sensitivity. Proc Natl Acad Sci U S A 2017;114:2705-10. - www.mitoeagle.org/index.php/Morrow_2017_Proc_Natl_Acad_Sci_U_S_A

Nicholls DG, Ferguson S. Bioenergetics 4. Elsevier 2013.

Paradies G, Paradies V, De Benedictis V, Ruggiero FM, Petrosillo G. Functional role of cardiolipin in mitochondrial bioenergetics. Biochim Biophys Acta 2014;1837:408-17. - http://www.mitoeagle.org/index.php/Paradies_2014_Biochim_Biophys_Acta

Pesta D, Hoppel F, Macek C, Messner H, Faulhaber M, Kobel C, Parson W, Burtscher M, Schocke M, Gnaiger E. Similar qualitative and quantitative changes of mitochondrial respiration following strength and endurance training in normoxia and hypoxia in sedentary humans. Am J Physiol Regul Integr Comp Physiol 2011;301:R1078–87.

Price TM, Dai Q. The Role of a Mitochondrial Progesterone Receptor (PR-M) in Progesterone Action. Semin Reprod Med. 2015;33:185-94.

1541 Prigogine I. Introduction to thermodynamics of irreversible processes. Interscience, New
1542 York, 1967;3rd ed.
1543 Puchowicz MA, Varnes ME, Cohen BH, Friedman NR, Kerr DS, Hoppel CL. Oxidative
1544 phosphorylation analysis: assessing the integrated functional activity of human skeletal
1545 muscle mitochondria – case studies. Mitochondrion 2004;4:377-85. -
1546 www.mitoeagle.org/index.php/Puchowicz_2004_Mitochondrion
1547 Puntschart A, Claassen H, Jostarndt K, Hoppeler H, Billeter R. mRNAs of enzymes involved
1548 in energy metabolism and mtDNA are increased in endurance-trained athletes. Am J
1549 Physiol 1995;269:C619-25.
1550 Quiros PM, Mottis A, Auwerx J. Mitonuclear communication in homeostasis and stress. Nat
1551 Rev Mol Cell Biol 2016;17:213-26.
1552 Reichmann H, Hoppeler H, Mathieu-Costello O, von Bergen F, Pette D. Biochemical and
1553 ultrastructural changes of skeletal muscle mitochondria after chronic electrical
1554 stimulation in rabbits. Pflugers Arch 1985;404:1-9.
1555 Renner K, Amberger A, Konwalinka G, Gnaiger E. Changes of mitochondrial respiration,
1556 mitochondrial content and cell size after induction of apoptosis in leukemia cells.
1557 Biochim Biophys Acta 2003;1642:115-23. -
1558 www.mitoeagle.org/index.php/Renner_2003_Biochim_Biophys_Acta
1559 Rich P. Chemiosmotic coupling: The cost of living. Nature 2003;421:583. -
1560 www.mitoeagle.org/index.php/Rich_2003_Nature
1561 Rostovtseva TK, Sheldon KL, Hassanzadeh E, Monge C, Saks V, Bezrukov SM, Sackett DL.
1562 Tubulin binding blocks mitochondrial voltage-dependent anion channel and regulates
1563 respiration. Proc Natl Acad Sci USA 2008;105:18746-51. -
1564 www.mitoeagle.org/index.php/Rostovtseva_2008_Proc_Natl_Acad_Sci_U_S_A

Rustin P, Parfait B, Chretien D, Bourgeron T, Djouadi F, Bastin J, Rötig A, Munnich A. Fluxes of nicotinamide adenine dinucleotides through mitochondrial membranes in human cultured cells. J Biol Chem 1996;271:14785-90.

Saks VA, Veksler VI, Kuznetsov AV, Kay L, Sikk P, Tiivel T, Tranqui L, Olivares J, Winkler K, Wiedemann F, Kunz WS. Permeabilised cell and skinned fiber techniques in studies of mitochondrial function in vivo. Mol Cell Biochem 1998;184:81-100. - http://www.mitoeagle.org/index.php/Saks_1998_Mol_Cell_Biochem

Salabei JK, Gibb AA, Hill BG. Comprehensive measurement of respiratory activity in permeabilized cells using extracellular flux analysis. Nat Protoc 2014;9:421-38.

Sazanov LA. A giant molecular proton pump: structure and mechanism of respiratory complex I. Nat Rev Mol Cell Biol 2015;16:375-88. - www.mitoeagle.org/index.php/Sazanov_2015_Nat_Rev_Mol_Cell_Biol

Schneider TD. Claude Shannon: biologist. The founder of information theory used biology to formulate the channel capacity. IEEE Eng Med Biol Mag 2006;25:30-3.

Schönfeld P, Dymkowska D, Wojtczak L. Acyl-CoA-induced generation of reactive oxygen species in mitochondrial preparations is due to the presence of peroxisomes. Free Radic Biol Med 2009;47:503-9.

Schrödinger E. What is life? The physical aspect of the living cell. Cambridge Univ Press, 1944. - www.mitoeagle.org/index.php/Gnaiger_1994_BTK

Schultz J, Wiesner RJ. Proliferation of mitochondria in chronically stimulated rabbit skeletal muscle--transcription of mitochondrial genes and copy number of mitochondrial DNA. J Bioenerg Biomembr 2000;32:627-34.

Simson P, Jepihhina N, Laasmaa M, Peterson P, Birkedal R, Vendelin M. Restricted ADP movement in cardiomyocytes: Cytosolic diffusion obstacles are complemented with a small number of open mitochondrial voltage-dependent anion channels. J Mol Cell Cardiol 2016;97:197-203. - PMID: 27261153

1591 Stucki JW, Ineichen EA. Energy dissipation by calcium recycling and the efficiency of
1592 calcium transport in rat-liver mitochondria. Eur J Biochem 1974;48:365-75.
1593 Tonkonogi M, Harris B, Sahlin K. Increased activity of citrate synthase in human skeletal
1594 muscle after a single bout of prolonged exercise. Acta Physiol Scand 1997;161:435-6.
1595 Waczulikova I, Habodaszova D, Cagalinec M, Ferko M, Ulicna O, Mateasik A, Sikurova L,
1596 Ziegelhöffer A. Mitochondrial membrane fluidity, potential, and calcium transients in
1597 the myocardium from acute diabetic rats. Can J Physiol Pharmacol 2007;85:372-81.
1598 Wagner BA, Venkataraman S, Buettner GR. The rate of oxygen utilization by cells. Free
1599 Radic Biol Med. 2011:51:700-712.
1600 http://dx.doi.org/10.1016/j.freeradbiomed.2011.05.024 PMCID: PMC3147247
1601 Wang H, Hiatt WR, Barstow TJ, Brass EP. Relationships between muscle mitochondrial
1602 DNA content, mitochondrial enzyme activity and oxidative capacity in man: alterations
1603 with disease. Eur J Appl Physiol Occup Physiol 1999;80:22-7.
1604 Watt IN, Montgomery MG, Runswick MJ, Leslie AG, Walker JE. Bioenergetic cost of
1605 making an adenosine triphosphate molecule in animal mitochondria. Proc Natl Acad Sci
1606 U S A 2010;107:16823-7. -
1607 www.mitoeagle.org/index.php/Watt_2010_Proc_Natl_Acad_Sci_U_S_A
1608 Weibel ER, Hoppeler H. Exercise-induced maximal metabolic rate scales with muscle aerobic
1609 capacity. J Exp Biol 2005;208:1635–44.
1610 White DJ, Wolff JN, Pierson M, Gemmell NJ. Revealing the hidden complexities of mtDNA
1611 inheritance. Mol Ecol 17; 2008:4925–42.
1612 Wikström M, Hummer G. Stoichiometry of proton translocation by respiratory complex I and
1613 its mechanistic implications. Proc Natl Acad Sci U S A 2012;109:4431-6. -
1614 www.mitoeagle.org/index.php/Wikstroem_2012_Proc_Natl_Acad_Sci_U_S_A
1615 Willis WT, Jackman MR, Messer JI, Kuzmiak-Glancy S, Glancy B. A simple hydraulic
1616 analog model of oxidative phosphorylation. Med Sci Sports Exerc. 2016;48:990-1000.